TALLINN UNIVERSITY OF TECHNOLOGY

FACULTY OF INFORMATION TECHNOLOGY

THOMAS JOHANN SEEBECK DEPARTMENT OF ELECTRONICS

BLOOD PULSE WAVEFORM MEASUREMENT FROM CAROTID ARTERIES USING BIOIMPEDANCE FOR INTRACRANIAL PRESSURE ASSESSMENT

Master thesis

Anton Kilk

Juhendaja: Rauno Gordon, PhD

Senior Research Scientist

Electronics and Bionics IAEM02/11

Tallinn 2014

TALLINNA TEHNIKAÜLIKOOL

INFOTEHNOLOOGIA TEADUSKOND

THOMAS JOHANN SEEBECKI ELEKTROONIKAINSTITUUT

BIOIMPEDANTSIGA VERE PULSILAINE KUJU MÕÕTMINE UNEARTERITE PEALT INTRAKRANIAALSE RÕHU HINDAMISEKS

Magistritöö

Anton Kilk

Juhendaja: Rauno Gordon, PhD

Vanemteadur

Elektroonika ja bioonika õppekava IAEM02/11

Tallinn 2014

I have written the Master's thesis independently.

All works and major viewpoints of the other authors, data from other sources of literature and elsewhere used for writing this paper have been referenced.

Master's thesis is completed under Rauno Gordon's supervision

Author A. Kilk .... (signature)

"......."....................201…..

Master's thesis is in accordance with terms and requirements "......."....................201….

Supervisor Rauno Gordon ….. (signature).

Accepted for defence

.... chairman of defence commission

"......."....................201… .

.... (signature)

3

ANNOTATSIOON

Võtmesõnad: aju, intrakraniaalne rõhk, vere pulsilaine, elektriline impedants, bioimpedants spektroskoopia.

Elektrilise bioimpedantsi (EBI) mõõtmine võib tulevikus olla kiireks ja mitteinvasiivseks meetodiks inimese organismi uurimisel. Siiamani on vähe uuritud võimalust südame pulsilaine impedantsi abil mõõta intrakraniaalse rõhu(ICP) muutumist peaajutraumade või muude patoloogiate korral.

Käesoleva töö käigus tutvustatakse ajuhaiguste erinevaid vorme ja intrakraniaalse rõhu erinevaid mõõtmismeetodeid. Praktilises osas uuritakse võimalust hinnata intrakraniaalset rõhku mõõtes vere pulsilaine kuju unearteri kohalt bioimpedants sagedusspektroskoobiga ning vastava meetodi kasutusala meditsiinis.

Töö on interdistsiplinaarne, suurema meditsiinilise kallakuga. Töös saadud tulemused võivad leida kasutust intrakraniaalse rõhu mitteinvasiivse uuringumeetodi arendamises.

TABLE OF CONTENTS

ABBREVIATIONS

BBB – Blood Brain Barrier

BMI – Body mass index

CBF – Cerebral Blood Flow

CNS - Central Nervous System

CPP – Cerebral Perfusion Pressure

CSF – Cerebral Spinal Fluid

CVR – Cerebrovascular Resistance

DBP – Diastolic Blood Pressure

EBI – Electrical Bioimpedance

ECG – Electrocardiography

ICG – Impedance Cardiography

ICH- Intracerebral Hemorrhage

ICP – Intracranial Pressure

MAP – Mean Arterial blood Pressure

ONSD - Optic Nerve Sheath Diameter

PEP – Pre-Ejection Period (in ECG terminology)

PI – Pulsatility Index

SBP – Systolic Blood Pressure

TCD - Transcranial Doppler Ultrasonography

TMD - Tympanic Membrane Displacement

TPR–Total Perpipheral Resistance (in medical terminology)

INTRODUCTION

This work is part of a cooperative project between the Tallinn Regional Hospital and Tallinn University of Technology called "The development of electrical tissues' diagnostic methods considering vascular system's dynamic forces". The purpose of the project is to achieve a better understanding of the vascular system's influence of different electrical diagnostic methods.

The monitoring of intracranial pressure (ICP) has been used for decades in the fields of neurosurgery and neurology. It is crucial for patient treatment to detect changes in ICP as early as possible, but the only option for the accurate measurement of ICP today is invasive measurement. However, there are certain limitations associated with invasive procedures:

— Additional risks to the patient, such as infection;

— High costs of the procedure;

— Limited resources, i.e., neurosurgeons and other qualified specialists.

This is the reason why alternative noninvasive methods for ICP assessment are in high demand today. The potential U.S. market for this product is approximately 2,5 billion US dollars [20]. In the North Estonian Regional Hospital there are around 200 patients per year who could benefit from this procedure.

Completely different from each other, by approach and complexity, ICP noninvasive measurement methods are being investigated on an ongoing basis. The most well-known of them are described in chapter 3, together with the invasive procedures. This work examines the possibility of using electrical bioimpedance (EBI) as a measurement tool of blood pulse waveform for ICP assessment.

The primary objective of this study is to answer the question: "Is it possible to obtain blood pulse waveform using EBI measurements on carotid arteries?"

This work consists of two parts – the theoretical and practical.

The theoretical objectives are:

— Get familiar with brain structure;

— Give an overview of different forms of brain traumas and pathologies;

— Give an overview of different ICP measurement methods;

The practical objectives are:

— Study the possibility of blood pulse measurement for ICP assessment;

— Perform repeated bioimpedance measurements of blood pulse waveform in the carotid arteries in which:

  o Compare electrodes' different placement configurations;

  o Compare measurements results at different frequencies;

  o Compare the measurement results between different individuals;

  o Make suggestions of best settings for future measurements.

This work is divided into four main parts. The first part called "General structures of the brain" giving an overview of brain anatomy. A description of the main brain parts and vessels is given.

The second part is called "Traumas and pathologies" and describes brain traumas or pathologies that can be related to increased ICP or changes in blood pulse waveform. The explanation of the relationship between ICP and intracranial volume is also presented.

The third part is called "Existing ICP measurement methods" and gives an overview of different ICP measurement methods.

The fourth part is called "ICP and Bioimpedance Measurements". In this chapter a method of ICP assessment using bioimpedance is described and conducted experiments are presented.

I.   GENERAL STRUCTURES OF THE BRAIN

1. Major Parts of the Brain

The adult brain consists of four major parts: brain stem, cerebellum, diencephalon, and cerebrum (Figure 1). The **brain stem** is continuous with the spinal cord and consists of the medulla oblongata, pons, and midbrain. Posterior to the brain stem is the **cerebellum** Superior to the brain stem is the **diencephalon** which as noted previously consists of the thalamus, hypothalamus, and epithalamus. Supported on the diencephalon and brain stem is the **cerebrum** the largest part of the brain [1]. There is an overview of major parts of the brain with their functions description in appendix 1.

Figure 1.The brain [1].
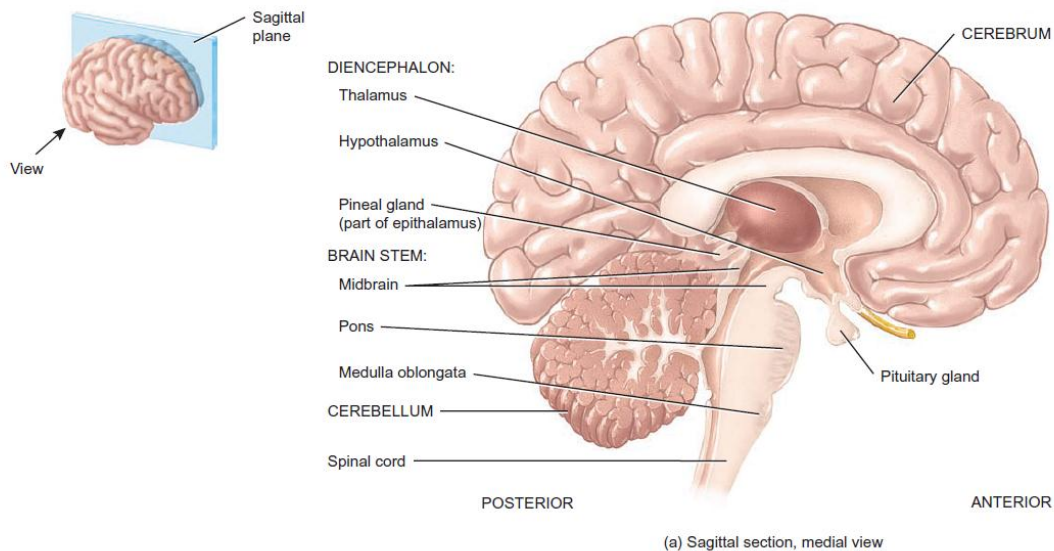
1.2 Protection and blood supply

1.2.1 Protective Coverings of the Brain

The cranium and the cranial meninges surround and protect the brain. The **cranial meninges** are continuous with the spinal meninges. They have the same basic structure, and bear the same names: the outer **dura mater**, the middle **arachnoid mater** and the inner **pia mater** (Figure 2a, b) [1, 2].

The **dura mater** is the outermost layer. It is primarily composed of tough, white, dense connective tissue and contains many blood vessels and nerves. It attaches to the inside of the cranial cavity and forms the internal periosteum of the surrounding skull bones [3].

The external layer is called the *periosteal layer* and the internal layer is called the *meningeal layer.* The two dural layers around the brain are fused together except where they separate to enclose the dural venous sinuses (endothelial-lined venous channels). These sinuses drain venous blood from the brain and deliver it into the internal jugular veins. The *epidural space* is a potential space between the periosteal layer of the dura mater and skull bones. Blood vessels that enter brain tissue pass along the surface of the brain; as they penetrate inward, the vessels become sheathed by a loose-fitting sleeve of pia mater. Three extensions of the dura mater separate parts of the brain. The **falx cerebri** separates the two hemispheres (sides) of the cerebrum. The **falx cerebelli** separates the two hemispheres of the cerebellum. The **tentorium cerebelli** separates the cerebrum from the cerebellum [1].
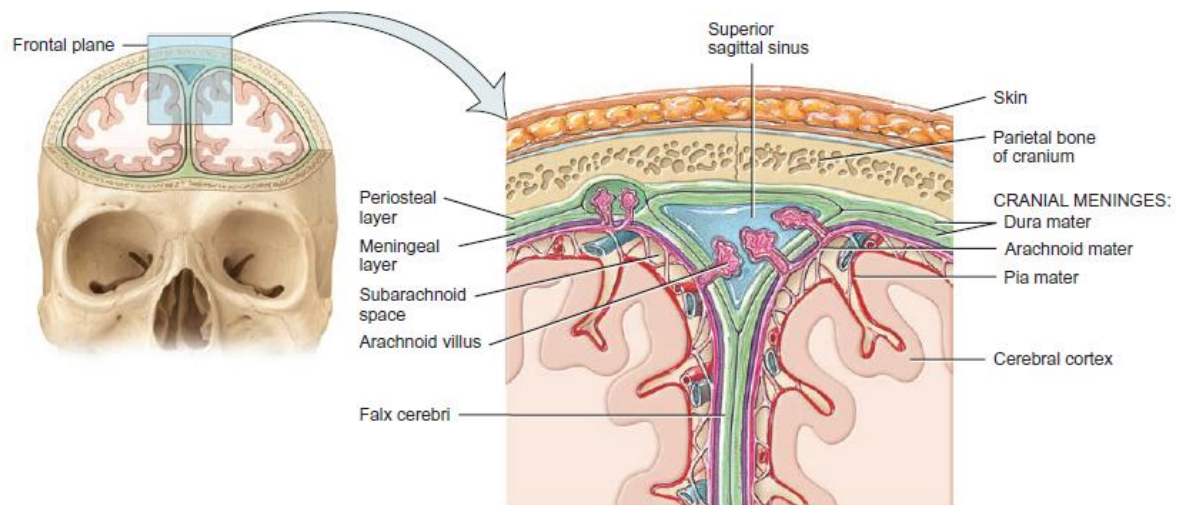

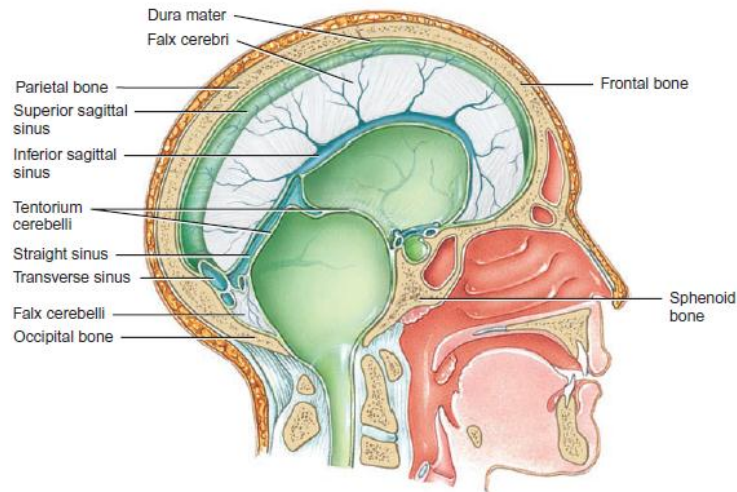*Figure 2a. The protective coverings of the brain. Anterior view [1].*

Figure 2b. Sagittal section of extensions of the dura mater [1].

1.2.2 Cerebrospinal Fluid

Cerebrospinal fluid (CSF) is a clear, colorless liquid comprised primarily of water that protects the brain and spinal cord against chemical and physical injuries. It also carries small amounts of oxygen, glucose, and other needed chemicals from the blood to neurons and neuroglia. CSF circulates slowly and continuously through cavities in the brain and spinal cord and around the brain and spinal cord in the subarachnoid space (space between the arachnoid mater and pia mater) [1].

Formation of CSF in the Ventricles

Figures 3a and b show the four CSF-filled cavities within the brain, which are called **ventricles.** There is one **lateral ventricle** located in each hemisphere of the cerebrum. Anteriorly, the lateral ventricles are separated by a thin membrane, the **septum pellucidum** (see Figure 4). The **third ventricle** is a narrow, slit-like cavity along the midline superior to the hypothalamus and between the right and left halves of the thalamus. The **fourth ventricle** lies between the brain stem and the cerebellum. The majority of CSF production is from the **choroid plexuses,** networks of modified blood capillaries in the walls of the ventricles (Figure 4).
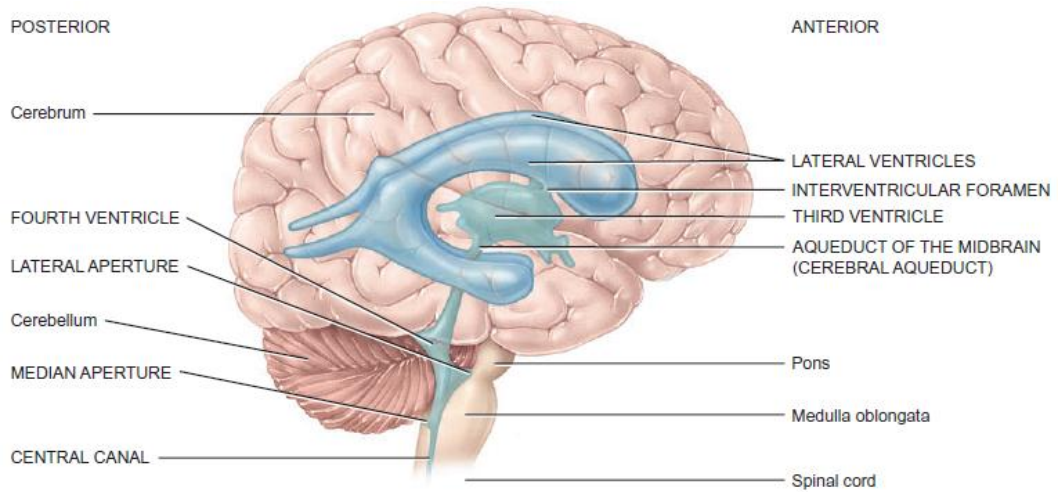
Figure 3a. Locations of ventricles.

The lateral ventricles connect by interventricular foramina to the third ventricle, and the aqueduct of the midbrain connects the third ventricle to the fourth ventricle.
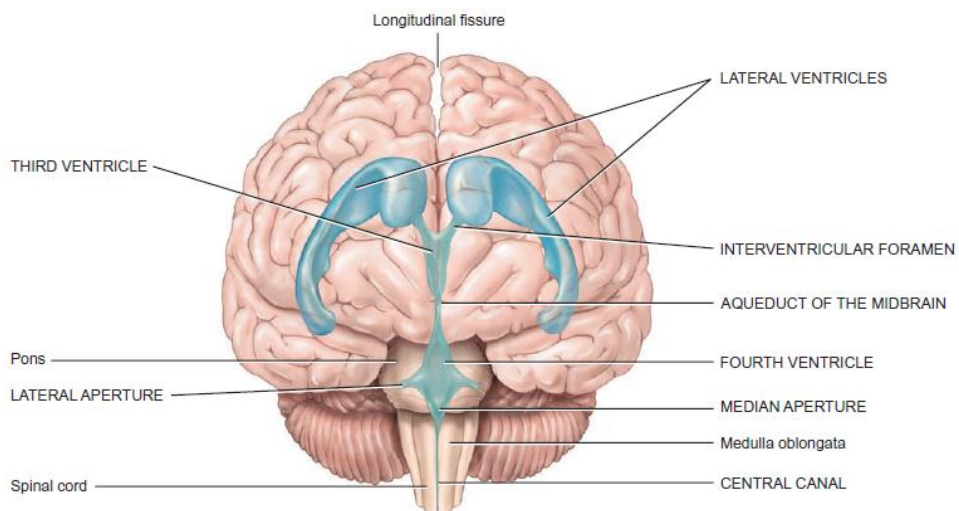

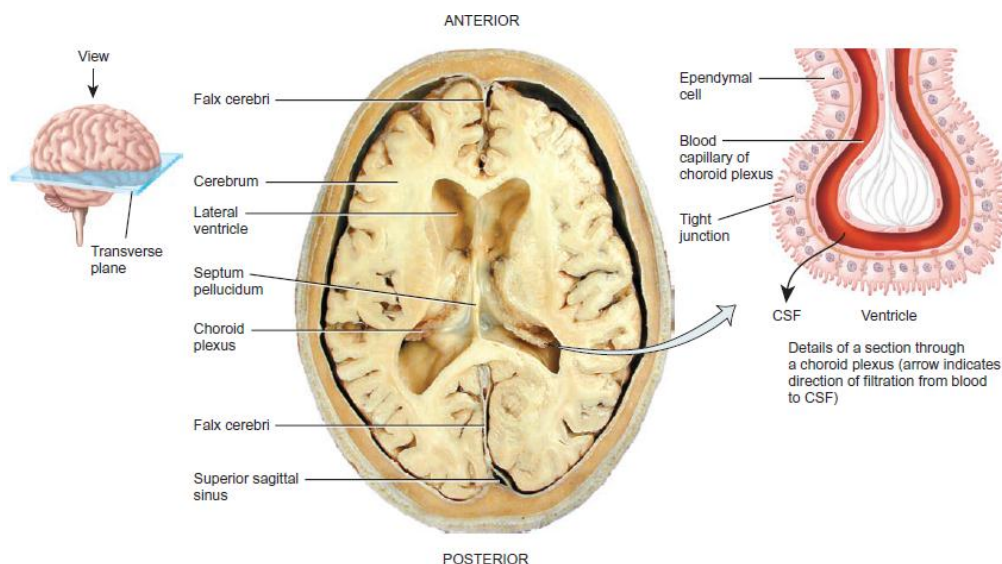*Figure 3b. Locations of ventricles.Anterior view.*

Figure 4. Superior view of transverse section of brain showing choroid plexuses.

Functions of CSF

The CSF functions in three main ways:

1. **Mechanical protection**. The primary function of the CSF is to serve as a shock-absorbing medium. It protects the delicate tissues of the brain and spinal cord from jolts that would otherwise cause them to hit the bony walls of the cranial cavity and vertebral canal. This important fluid also buoys the brain so that it "floats" in the cranial cavity and reduces its weight within the skull to approximately 50 grams [1].

2. **Chemical protection**. CSF provides an optimal chemical environment for efficient neuronal signaling. Even slight changes in the ionic composition of CSF within the brain can seriously disrupt production of action potentials [1].

3. **Circulation**. CSF is a medium for the minor exchange of nutrients and waste products between the blood and adjacent nervous tissue. The subarachnoid space through which CSF flows is continuous with the perivascular spaces (spaces around the blood vessels that penetrate the brain tissue); together, the CSF and these spaces provide a lymphatic function for the tissue of the brain [1].

1.2.3 Brain Blood Flow and the Blood–Brain Barrier

Blood flows to the brain mainly via the **internal carotid** and **vertebral arteries** (see Figure 6a, b); the dural venous sinuses drain into the internal jugular veins to return blood from the head to the heart (see Figure 7) [1].

The **blood–brain barrier (BBB)** consists mainly of tight junctions that seal together the endothelial cells of brain blood capillaries and a thick basement membrane that surrounds the capillaries [1].
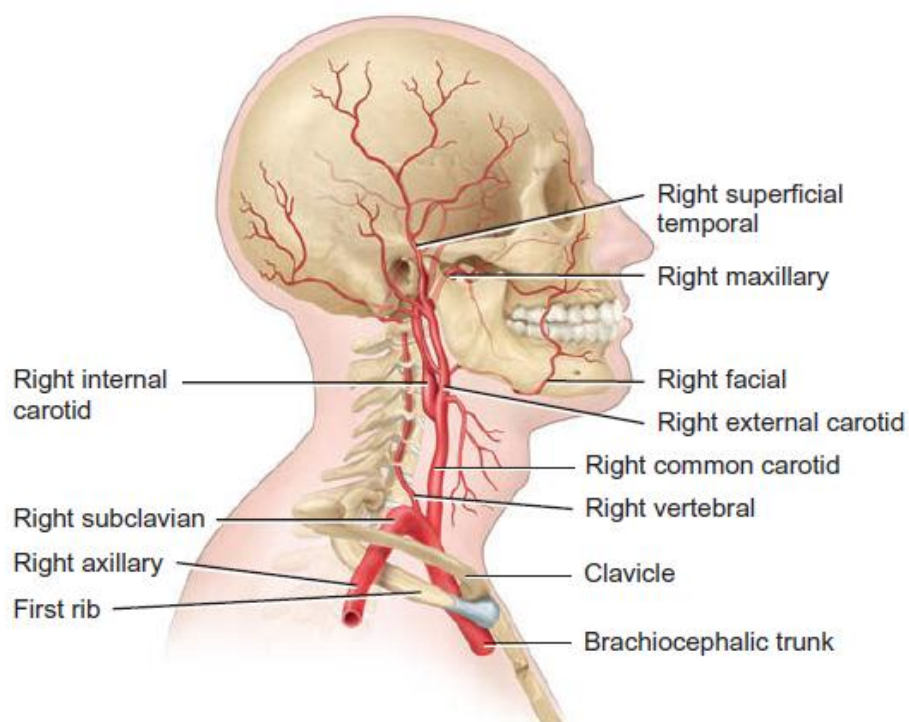

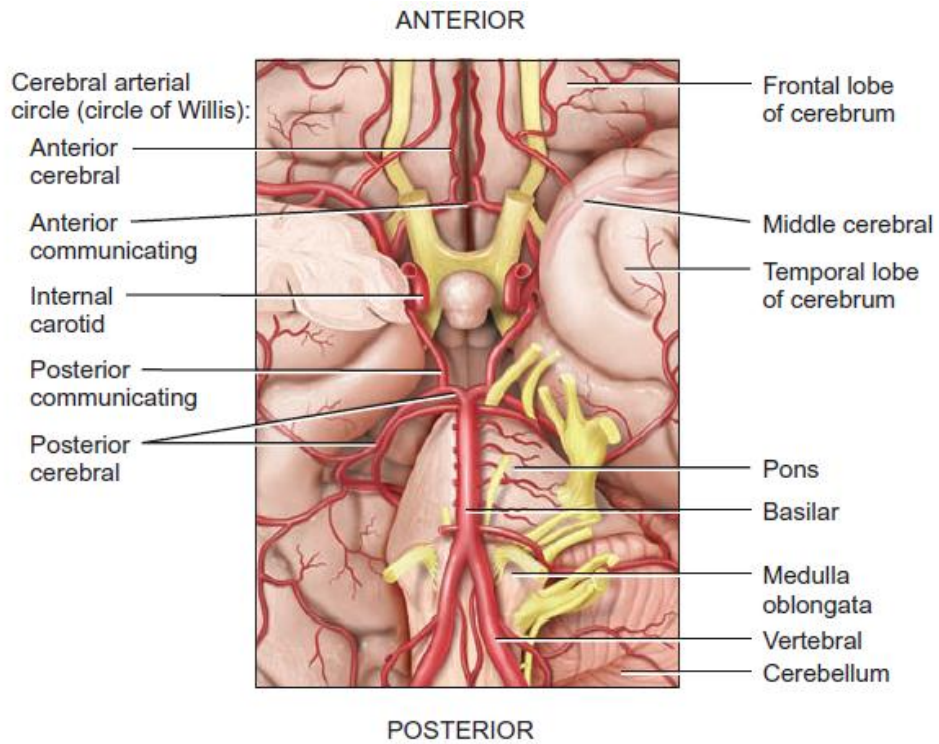*Figure 6a. Right lateral view of branches of brachiocephalic trunk in neck and head.*

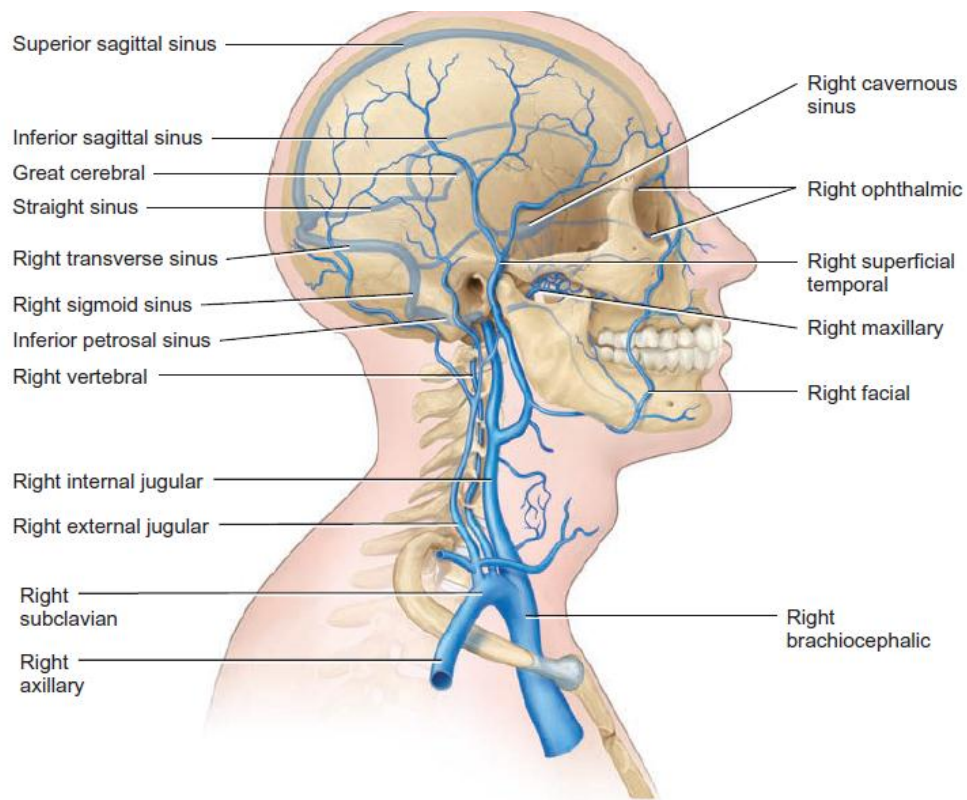*Figure 6b. Inferior view of base of brain showing cerebral arterial circle.*

Figure 7. Principal veins of the head and neck.

II. TRAUMAS AND PATHOLOGIES

2.1 The Monro-Kellie hypothesis

The Monro-Kellie hypothesis describes the relationship between ICP, volume of CSF, blood and brain tissue. It states on the proposals of Scottish anatomist Alexander Monro, that:

1) The brain is encased in a rigid structure;

2) The brain is incompressible;

3) The volume of the blood in the cranial cavity must therefore be constant;

4) A constant drainage of venous blood is necessary to make room for the arterial supply.

In 1926, Harvey Cushing, American neurosurgeon, formulated the doctrine as we know it today, namely, that **with an intact skull, the volume of the brain, blood, and CSF is constant**. **An increase in one component will cause a decrease in one or both of the other components** [11]. This statement is used as basis   in practical part of this work, where intracranial blood pressure level changing is considered to be indicator for ICP level changing.

A relationship between intracranial pressure and volume is shown on Figure 8. It is found that CSF volume is **60–80 mL** in young persons and **100–140 mL** in elderly, mainly due to cerebral atrophy. Normal ICP varies with age and body posture but is generally considered to be **5–15mmHg** in healthy supine adults, **3–7mmHg** in children and **1,5–6mmHg** in infants [11].
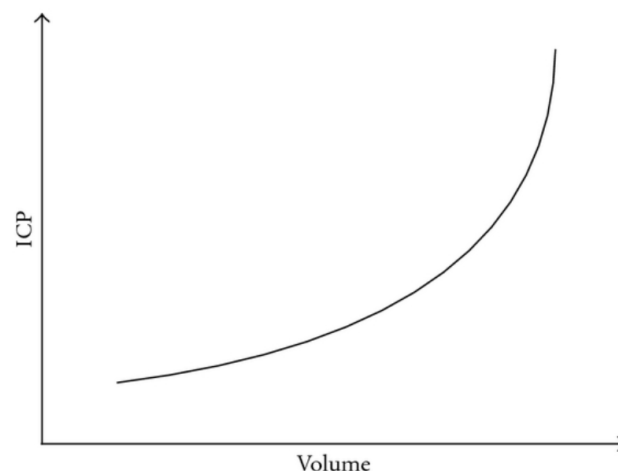

Figure 8. The relationship between intracranial pressure and volume [11].

2.2 Elevated ICP, brain traumas and pathologies

Elevated ICP can be the cause of crushed brain tissue as well as its consequence. The brain takes approximately 90% of intracranial volume, with the remaining 10% blood and CSF. Trauma or some pathology like tumor or aneurysm increases brain's proportions as well as ICP. Not significant at the beginning, further volume increase causes an exponential ICP grow as it is shown at Figure 8. The consequences are shifts of brain tissue, new traumas and other pathologies described below in this chapter. As a rule, an ICP level of 25-40 mmHg is tolerated well by human. At ICP level of 40-50mmHg loss of consciousness can happen due to ischemia of brain tissues. In this case oxygen cannot reach brain by cerebral arteries as their pressure is approximately the same level. Early detection and identification of cause of elevated ICP can be life saving.

Thought not every trauma or pathology related to changes in ICP, some of the factors of disease, like decreased distensibilty of intracranial arteries or increased total peripheral resistance(TPR) can be noticed from changes in arterial blood wave's shape [5]. This fact gives us the reason to describe briefly in this chapter all the potential brain diseases and pathologies, that could benefit from using the blood pulse shape measurement method for pathology diagnostics. They are divided into:

1) **diseases related to tumors and increased ICP;**
2) **brain traumas;**
3) **cerebrovascular diseases;**
4) **brain infections and autoimmune diseases.**

Brain pathologies linked to neurogenerative conditions, toxic and metabolic disorders are not described here as they are not directly related to changes in ICP. Thought some of them could also be investigated measuring carotid arteries' pulse shape.

2.3 Diseases related to tumors and increased ICP

2.3.1 Herniations

Brain herniation is a shift of the brain within the scull. Usually it is a consequence of high ICP. There are different types of herniation existing (Figure 9). The most common are: cingulate (subfalcine), uncal, central and cerebellar tonsillar [6].
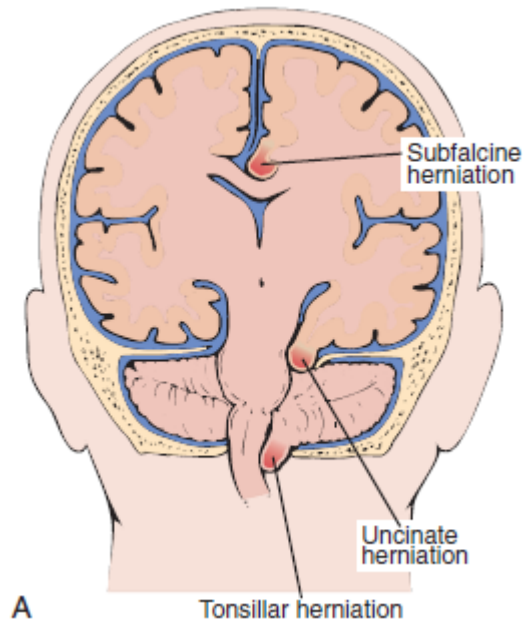
Figure 9.Types of herniations [6].

2.3.2 Cerebral edema

Cerebral edema is an absolute increase in brain water content. The amount of water in brain tissue is tightly controlled by the production of CSF, rate of egress of CSF from the cranial vault and flux of water across the blood-brain barrier. The blood brain barrier separates the brain from the blood so that only lipid-soluble molecules, or molecules that can access specialized transport systems, enter the brain. The structural basis of the blood-brain barrier is endothelial cell tight junctions lining the cerebral vessels. Water can enter the brain uncontrollably if the barrier is disrupted or if osmotic forces across the barrier are sufficient to drive water into the cerebral tissues [6].

2.3.3 Hydrocephalus

Hydrocephalus is accumulation of CSF within the ventricles resulting in dilatation of these structures (Figure 10). Accumulation of CSF can arise from one of two processes:

- overproduction of CSF, which is very rare, occurring only in the context of tumors of the choroid plexus;
- Failure of CSF egress from the cranial vault, which is the most common mechanism [6].
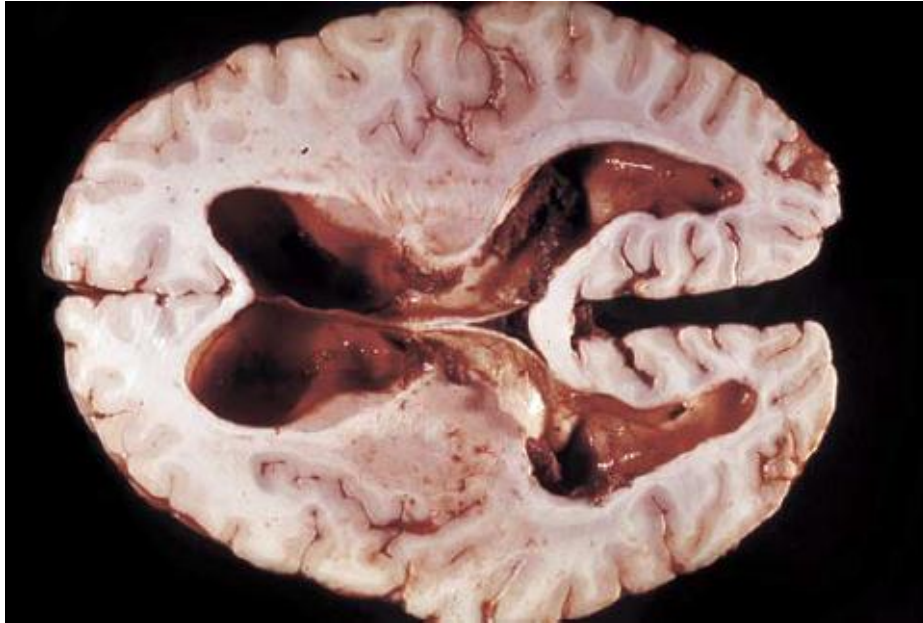
Figure 10. Hydrocephalus [6].

Horizontal section of the brain from a patient who died of a brain tumor that obstructed the aqueduct of Sylvius shows marked dilation of the lateral ventricles [6].

2.3.3 Central Nervous System Neoplasia (Tumors)

Neoplasm is an abnormal growth or division of cells in different tissues, which can be divided into benign and malign forms. Primary CNS cancers account for about 1.5% of all primary malignant tumors. Over 130 different types of CNS neoplasms are recognized and formally codified by the World Health Organization, but most are very rare. By far the most common are meningiomas and gliomas, each of which accounts for about one third of all CNS tumors (Table 1) [6].

Table 1

Major Types of Primary Central Nervous System (CNS) Tumors [6]

Meningioma
Gliomas
Medulloblastoma and other primitive neuroectodermal tumors
Craniopharyngioma
Germ cell tumors
Hemangioblastoma
Neuronal and mixed glioneuronal tumors
Pineal tumors
Primary CNS lymphoma

2.4 Brain traumas

Physical injury of the brain, spinal cord and peripheral nervous system constitutes a major cause of loss of life and productivity. Populations at highest risk for such injuries include children, men in late adolescence and early adult life, and the elderly [6].

2.4.1 Epidural Hematoma

Epidural hematoma is an intracranial buildup of blood between the dura mater and the skull caused by head injury (Figure 11).

Epidural hematoma usually results from a blow to the head with skull fracture and, unless treated promptly, can be fatal. It occurs in 1% to 2% of head injuries [6].
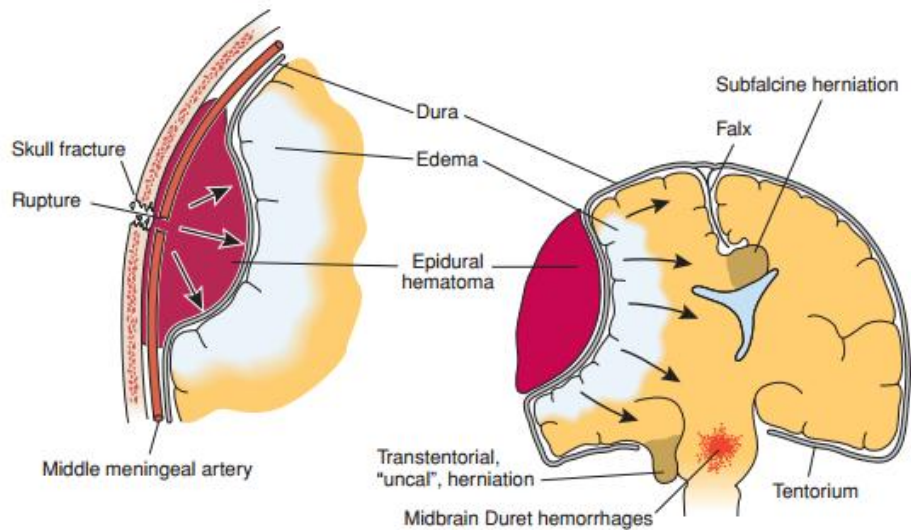
Figure 11. Development of an epidural hematoma [6].

Laceration of a branch of the middle meningeal artery by the sharp bony edges of a skull fracture initiates bleeding under arterial pressure that dissects the dura from the calvaria and produces an expanding hematoma [6].

2.4.2 Subdural hematoma

Subdural hematoma (Figure 12) is a buildup of blood between the dura mater and the brain tissue. Subdural hematoma is a significant cause of death after head injuries from falls, assaults, vehicular accidents and sporting mishaps. The hematomas expand more slowly than an epidural hematoma, so the clinical tempo is slower, but once critical increased ICP is attained, clinical deterioration and death can occur rapidly [6].

Figure 12. Development of a subdural hematoma [6].

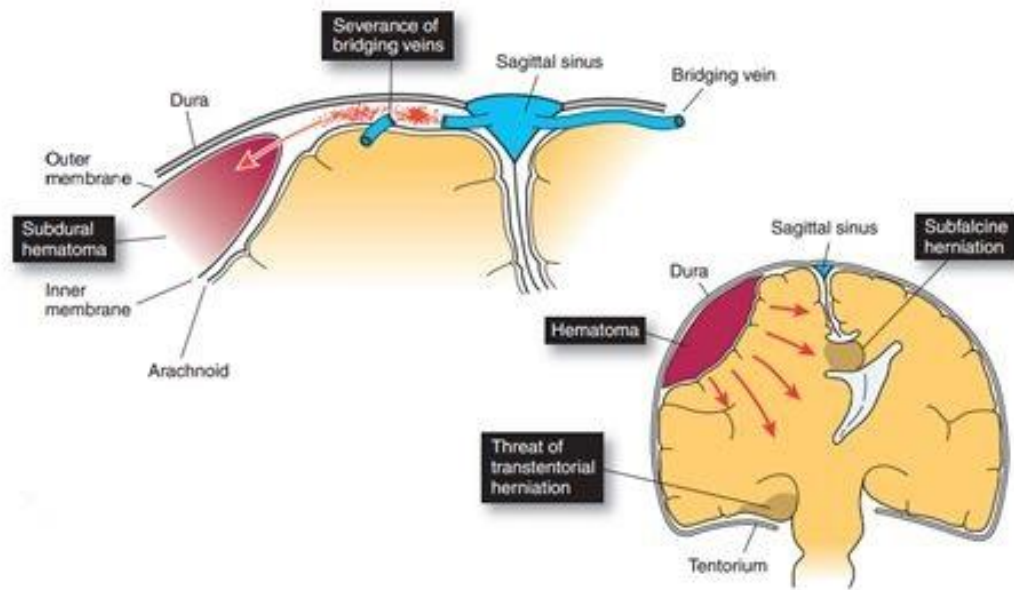*With head trauma, the dura moves with the skull, and the arachnoid moves with the cerebrum. As a result, the bridging veins are sheared as they cross between the dura and the arachnoid. Venous bleeding creates a hematoma in the expansile subdural space [6].*

2.4.3 Concussion

Concussion is a transient loss of consciousness caused by biomechanical forces acting on the CNS. The classic example of concussion occurs in the boxing ring as the consequence of a blow that deflects the head upward and posteriorly, often with a rotatory component. Recent advances in imaging suggest that axonal injury and disconnection may account for cognitive and memory difficulties, vertigo and feelings that "things are just not quite right" that bedevil individuals with "mild" traumatic brain injury [6].

2.4.4 Cerebral Contusion

A cerebral contusion (Figure 13) is a more severe form of traumatic brain injury with multiple microhemorrages in the brain tissue and can be a life threatening condition. The treatment aims to prevent dangerous rises in intracranial pressure [5].
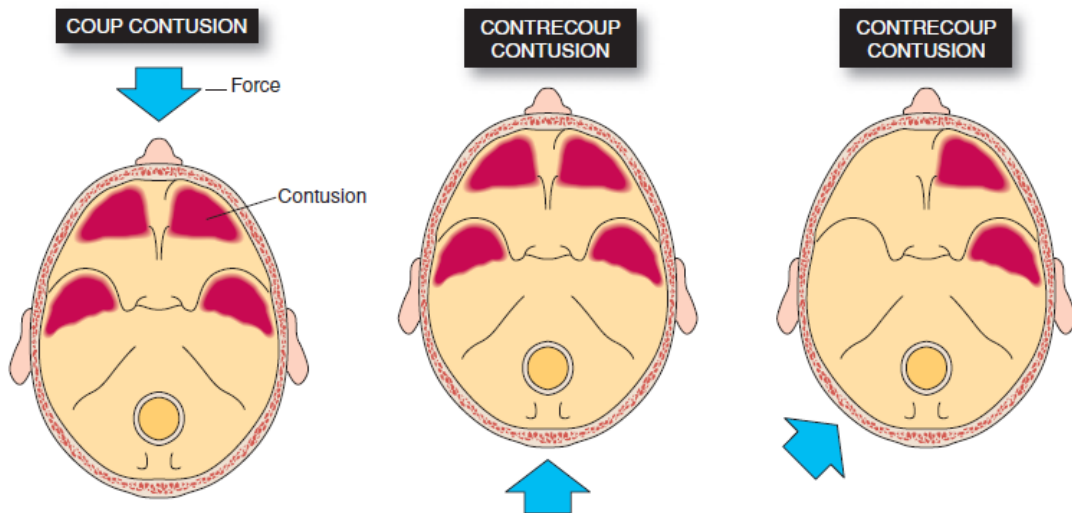
Figure 13. Biomechanics of cerebral contusion [6].

The cerebral hemispheres float in the cerebrospinal fluid. Rapid deceleration or acceleration of the skull causes the cortex to impact forcefully into the anterior and middle fossae. The position of a contusion is determined by the direction of the force and the intracranial anatomy.[6]

2.4.5 Penetrating Traumatic Brain Injury

Penetrating objects such as bullets and knives enter the cranium and traverse the brain with variable velocities (Figure 14). In the absence of direct damage to the vital brain centers, the immediate threat to life is hemorrhage [6].

Figure 14. Consequences of high- and low-velocity bullet wounds [6].

A. The "blast effect" of a high-velocity projectile causes an immediate increase in supratentorial pressure and results in death because of impaction of the cerebellum and medulla into the foramen magnum. B. A low-velocity projectile increases the pressure at a more gradual rate through hemorrhage and edema [6].
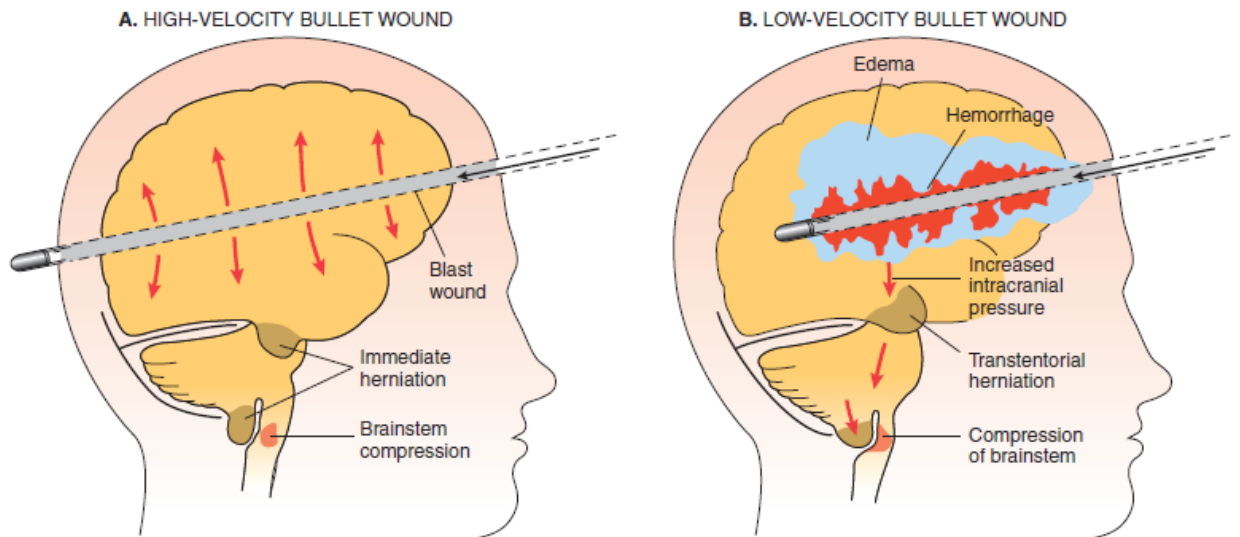
2.5 Cerebrovascular disorders

Stroke is the third leading cause of death after myocardial infarction and cancer. As elsewhere, vascular disease can result from either vessel blockage, causing ischemia, or leaking of the vessels, resulting in hemorrhage [6].

2.5.1 Stroke

Stroke is the rapid loss of brain function due to disturbance in the blood supply to the brain. This can be due to ischemia (lack of blood flow) caused by blockage (thrombosis, arterial embolism) or a hemorrhage. As a result, the affected area of the brain cannot function, which might result in an inability to move one or more limbs on one side of the body, inability to understand or formulate speech, or an inability to see one side of the visual field [8].

2.5.2 Ischemic stroke

In an ischemic stroke (Figure 15), blood supply to part of the brain is decreased, leading to dysfunction of the brain tissue in that area. There are four reasons why this might happen:

1. Thrombosis (obstruction of a blood vessel by a blood clot forming locally)
2. Embolism (obstruction due to an embolus from elsewhere in the body)
3. Systemic hypoperfusion (general decrease in blood supply, e.g., in shock)
4. Venous thrombosis [8].
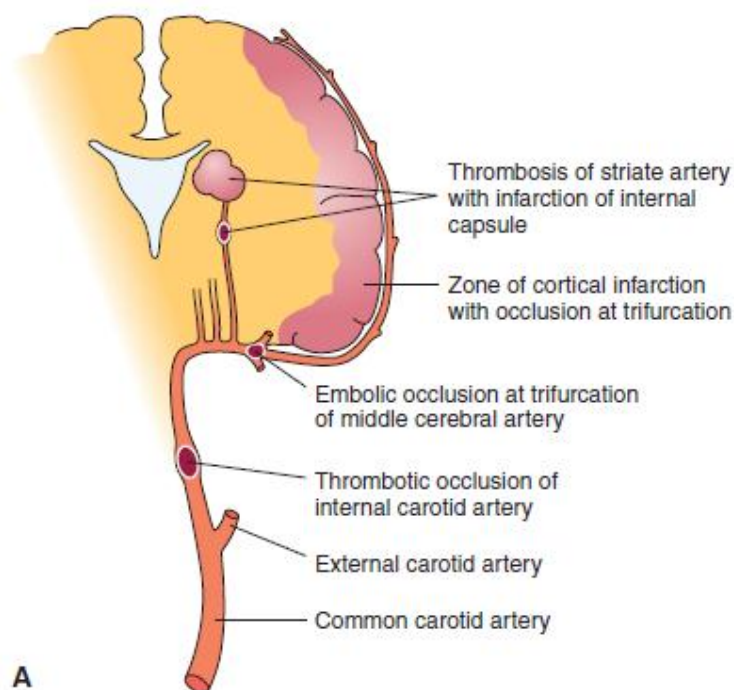
Figure 15. Distribution of cerebral infarcts [6].

The normal distribution of the cerebral vasculature defines the pattern and size of infarcts and, consequently, their symptoms. Occlusion at the trifurcation causes cortical infarcts with motor and sensory loss and often aphasia. Occlusion of a striate branch transects the internal capsule and causes a motor deficit [6].

2.5.3 Hemorrhagic stroke

Hemorrhagic stroke is a bleeding of blood vessels of the brain that causes blood accumulation and compression of the surrounding brain tissue. This can distort and injure

tissue. In addition, the pressure may lead to a loss of blood supply to affected tissue with resulting infarction, and the blood released by brain hemorrhage appears to have direct toxic effects on brain tissue and vasculature. Inflammation contributes to the secondary brain injury after hemorrhage [8]. It can be divided into two types of intracerebral hemorrhage (Figure 17) or subarachnoid hemorrhage.

Cerebral hemorrhages that occur without trauma are usually caused by vascular malformations or are consequences of long-standing hypertension (Figure 17).
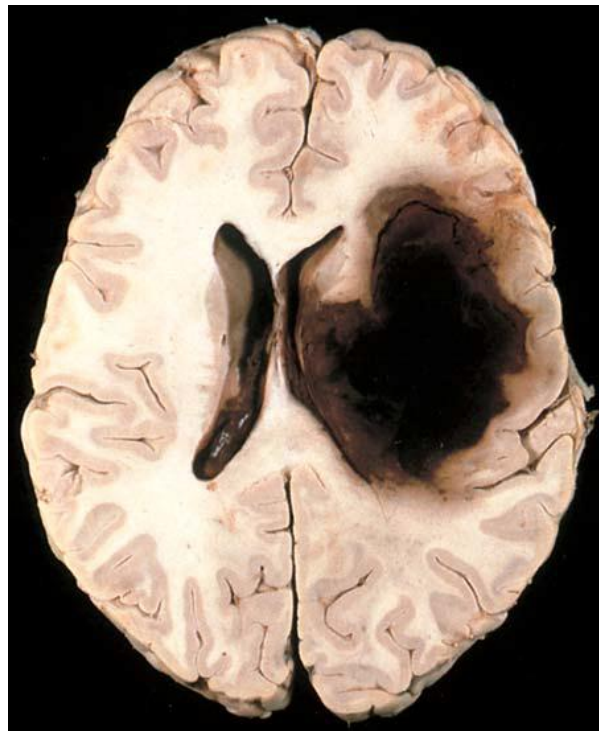
Figure 17. Intracerebral hemorrhage in the basal ganglia [6].

A hypertensive patient bled into the basal ganglia, resulting in acute severe headache, contralateral hemiparesis and rapid decline in level of consciousness. The deep cerebral nuclei (basal ganglia) and thalamus are the most common locations of intracerebral hemorrhages [6].

Intravascular pressure and weakness in arterial walls lead to formation of cerebral aneurysms that may rupture, leading to subarachnoid hemorrhage [6]. Aneurysm is a dilatation of blood vessel that is often forming a pulsating tumor (Figure 18).

Figure 18. Angiograph of an aneurysm in a cerebral artery [9].

2.6 Infectious disorders

Brain diseases in the category of infections include:

Meningitis: An inflammation of the lining around the brain or spinal cord, usually due to infection. Neck pain, headache, and confusion are common symptoms.

Encephalitis: An inflammation of the brain tissue, usually due to infection. Meningitis and encephalitis often occur together, which is called meningoencephalitis.

Brain abscess: A pocket of infection in the brain, usually caused by bacteria. Antibiotics and surgical drainage of the area are often necessary [4].

Many of the infections of the nervous system are devastating or lethal if untreated [6].

2.7 Idiopathic intracranial hypertension

Idiopathic intracranial hypertension, also called pseudotumor cerebri, is a unique syndrome of relatively severe poorly defined and often progressive headaches with associated horizontal diplopia ("double vision"). In addition, transient visual obscurations and pulsatile tinnitus ("ringing of the ears") may be part of the clinical picture [10].

III. EXISTING ICP MEASUREMENT METHODS

Monitoring of intracranial pressure (ICP) has been used for decades in the fields of neurosurgery and neurology. It is crucial for patient treatment to detect changes in ICP as early as possible. There are multiple techniques: invasive as well as noninvasive (see Table 2). All these methods are shortly described in this chapter.

Table 2

ICP monitoring methods compared [11]

Technology	Accuracy	Rate of infection	Rate of hemorrhaging	Cost per patient	Miscellaneous
External ventricular drainage	High	Low to moderate	Low	Relatively low	Can be used for CSF and infusion of antibiotics
Microtransducer ICP monitoring devices	High	Low	Low	high	Some transducers have problems with high zero drift
Transcranila Dopler ultrasonography	Low	None	None	Low	High percentage of unsuccesful measurements
Tympanic membrane displacement	Low	None	None	Low	High percentage of unsuccesful measurements
Optic nerve Sheath diameter	Low	None	None	Low	Can potentially be used as a screening method of detecting raised ICP
MRI/CT	Low	None	None	Low	MRI has potential for being used for noninvasive estimation of ICP
Fundoscopy (papilledema)	Low	None	None	Low	Can be used as a screening method of detecting raised ICP, but not in cases of sudden raise of ICP, that is trauma

External ventricular drainage is considered the gold standard in terms of accurate measurement of pressure, although microtransducers generally are just as accurate [11].

The non-invasive techniques are without the invasive methods' risk of complication, but fail to measure ICP accurately enough to be used as routine alternatives to invasive measurement. Raboel et al (2012) concluded, that "Invasive measurement is currently the only option for accurate measurement of ICP" [11].

However, there are certain limitations associated with invasive procedures:

— additional risks to the patient, such as infection;

— high costs of the procedure;

— limited resources, i.e., neurosurgeons and other qualified specialists.

This is the reason why alternative noninvasive methods for ICP assessment are highly demanded today.

3.1. External Ventricular Drainage (EVD)

This technique involves the introduction of the catheter in the patient's skull. Procedure is usually performed by neurosurgeons or specialists in the field of neurology and requires proper infrastructure and qualified staff. In addition to measuring ICP, this technique can also be used for drainage of CSF and administering of medicine intrathecally, for example, antibiotic administration. There may be some complications related to the EVD. During long-term CSF drainage compression of the ventricular system may arise and blocks proper EVD drainage. Additionally, EVD placement may be indicated to drain posttraumatic hemorrhage [11].

3.2 Microtransducer ICP Monitoring Devices

This is invasive procedure, which includes the introduction of microsensor into the brain of patient. Microsensors or transducers are divided by functionality into fiber optic devices, strain gauge devices, and pneumatic sensors.

Fiber optic devices transmit light via a fiber optic cable towards a displaceable mirror. Changes in ICP will move the mirror, and the differences in intensity of the reflected light are translated to an ICP value. Strain gauge devices use piezoelectric sensors. With changing of pressure inside the skull, transducer is bent and deformation changes the resistance of sensor. Resistance value is then translated to ICP value. Pneumatic sensors are called so, because they use a small balloon, which is placed in the distal end of the catheter. The pressure inside the balloon is known, so the intracranial pressure can be calculated. This technique additionally allows quantitative measurement of intracranial compliance. Complications are possible as with ventricular drainage, mainly the risk of hemorrhage and infection. Some of the sensors contain ferromagnetic components and therefore patients with these devices cannot undergo MRI. Generally, microtransducers

show the same level of accuracy as EVD, but most of them have common disadvantage - it is not possible recalibrate them after placement and zero reference drift can happen [11].

3.3 Transcranial Doppler Ultrasonography (TCD)

The TCD technique involves ultrasound waves' radiation through patient's skull for determining blood flow velocity in cerebral vessels. The difference between systolic and diastolic flow velocity, divided by the mean flow velocity, is called the pulsatility index (PI):

$$PI = \frac{\text{systolic flow velocity} - \text{diastolic flow velocity}}{\text{mean flow velocity}} \tag{1}$$

PI is found to correlate with invasively measured ICP and correlation coefficients between 0,439 and 0,938 have been found. The problem is that at high ICP values the deviation magnitude grows significantly and accuracy becomes unacceptable for clinic measurements [11].

3.4 Tympanic Membrane Displacement (TMD)

TMD involves a catheter insertion inside the patient's ear to stimulate the stapedius muscle. Stimulation of the stapedial reflex causes a movement of the tympanic membrane (Figure 19), which is shown to correlate to ICP. However, the measurements applied to different subjects suffer the accuracy, which precludes this method to use clinically [11].
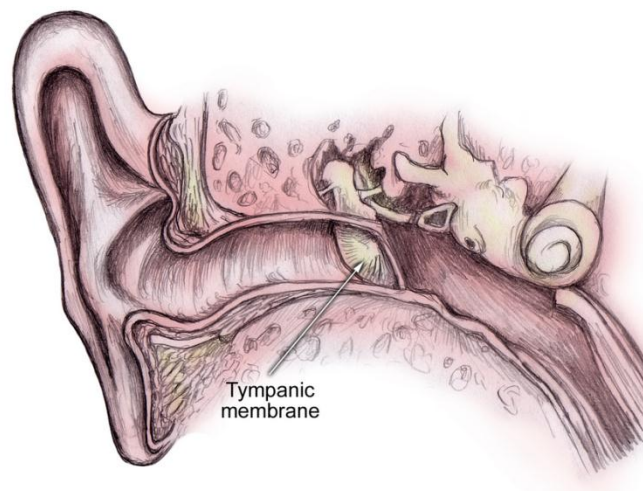

Figure 19. Tympanic membrane [12].

3.5 Optic Nerve Sheath Diameter (ONSD)

ONSD implies the use of ocular ultrasound for visualizing changes in optic nerve (Figure 20) sheath diameter. The optic nerve is surrounded by the dural sheath. In cases of increased ICP, the sheath expands [11].
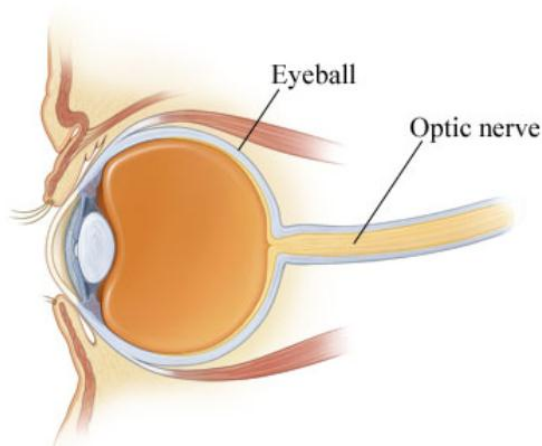

Figure 20. Optic nerve [13].

At the moment this technique lacks accuracy to replace invasive ICP measuring methods, but can be used to distinguish between normal and increased (>20 mmHg) ICP [11].

3.6 Magnetic Resonance Imaging (MRI) & Computer Tomography (CT)

MRI and CT are often applied in clinical practice to determine a brain trauma or pathology. Previous studies show that these techniques are not effective in ICP monitoring. No method of estimating ICP on the basis of cranial CT scans currently exists [11].

If we accept some shortcomings, MRI can be used as a method of determining the need of ICP monitoring for patient with moderate head trauma [11].

3.7 Fundoscopy and Papilledema

Papilledema is optic disc swelling that is caused by increased ICP can be visualized by fundoscopy – a method of eye examination. The technique is limited to the abilities of examiner as well as the circumstances surrounding the examination. Furthermore, the process is considered as time consuming and cannot be applied in emergency situations [11].

IV. ICP AND BIOIMPEDANCE MEASUREMENTS

4.1 The relation between ICP and blood pulse waveform.

The idea of investigating relation between blood pulse waveform and ICP has been proposed on a meeting related to project called "The development of electrical tissues' diagnostic methods considering vascular system's dynamic forces". The purpose of which, as it was mentioned before, was to achieve better knowledge of the vascular system's influence for different electrical diagnostic methods. The assumption of existing relation was based on theory of reflected waves in closed cavities. As blood impulse travels from heart to blood vessels of the brain, it partially reflects from some bifurcations and constrictions of vessels. It was proposed, that investigating these reflections at measurement points – neck vessels, could give us information about changes of pressure inside the scull. Further studies in this area brought us to confirmation of this theory in previously performed studies.

The Monro-Kellie hypothesis that was described closely in chapter 2.1 shows the relationship between intracranial pressure and volume [11].

Marmarou et al [18] first introduced the principles of cerebral hemodynamics. They showed theoretically and experimentally, that knowing four parameters the pressure response to a known volume change can be predicted. These parameters are:

1) The rate of CSF production;
2) The variable compliance given by the exponential relationship of ICP to volume;
3) The outflow resistance;
4) The intradural sinus pressure;

Considering listed studies we could bring here next outcomes related to purpose of this works:

1) There is a non-linear, monotonic relationship between ICP and intracranial volume.
2) The energy of the reflected blood wave in intracranial vessels is inversely proportional to intracranial compliance (dP/dV) and therefore, via this volume/pressure relationship could be indicative of ICP.
3) Performing an observation of patient and knowing particular parameters, we can predict his/her ICP value non-invasively, following changes in reflected blood wave.

Considering these statements above, next questions should be asked:

1) What blood vessels could be the best to observe changes in reflected wave?

2) What technology is the best for observing these changes?

Anatomically, the most "comfortable" measurements could be applied on carotid arteries as these are the largest vessels that transport blood into brain. Carotid arteries are also one of the common palpable sites for heart pulse measurement.

One of the solutions regarding the technology is proposed by Svoboda et al [14]. This technology uses pressure sensor positioned against the palpable carotid artery to detect ICP. This technology is described in next chapter.

4.2 Measurements using pressure sensors

It appears that first attempts to obtain blood pulse wave for ICP measurements were done by Svoboda et al [14]. They patented a system and method for non-invasively detecting ICP by detecting impedance mismatches between carotid arteries and cerebral vessels using a pressure sensor positioned against the palpable carotid artery.

They found that there was a strong, highly linear relationship identified between leg elevation (a surrogate for ICP elevation) and time delay between the systolic maximum and the dicrotic notch, a parameter designed as *X3* (Figure 21).

According to cardiac cycle parameter *X3* is a period between the moment, when maximum systolic flow occurs and the moment of aortic valve closing in the same cardiac cycle.
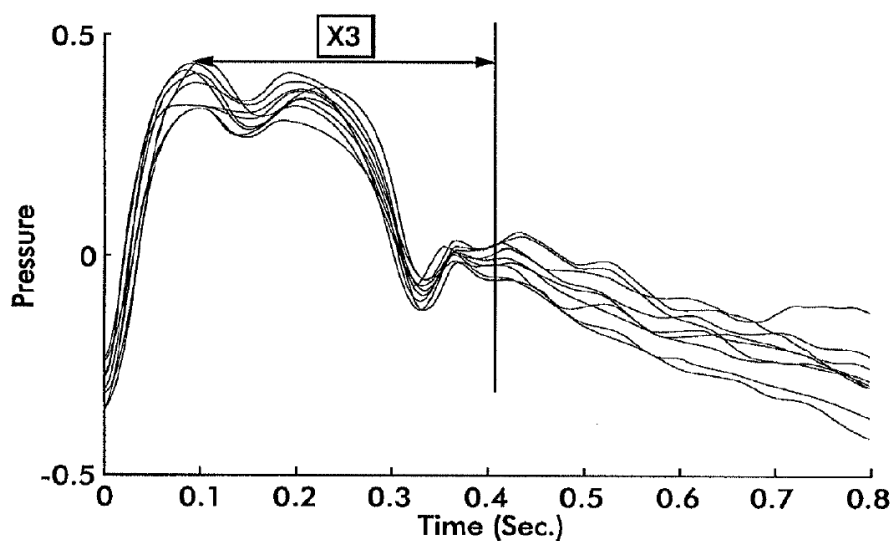

Figure 21. Averaging of pulse waveforms collected over time to produce a "typical" representative waveform for future mining [14].

Reference sensor

In vivo measurements showed that proposed method for deriving ICP could be too strongly influenced by the other parameters of the circulatory system, producing unreliable results. In this case a reference pulse proposed to be utilized (Figure 22), collected at a "control" artery (such as the radial artery pulse, or any other artery remote from the carotid artery), to compensate for systematic impedance.

It is worth to examine this solution for extracting ICP data from systematic impedance as it possibly can be combined with EBI measurements. Authors propose at least two types of reference measurements – tonometry sensor (pressure sensor, same as used on carotid artery) or optical plethysmography (in this case, a reference signal recorded on the index finger). Both methods are used to register blood pulse wave in circulatory system at long distance from carotid artery. The data from both sites is then compared and ICP data is extracted. In case of plethysmography it is suggested to use derivatives' maxima and minima for time differences calculation [14].

It is not excluded that we can use reference signal with EBI measurements. Moreover, analyzing pulse derivatives (as it is done using optical plethysmography) from two measurement sites, separated anatomically can facilitate the obtaining of ICP phenomena from blood impulse.
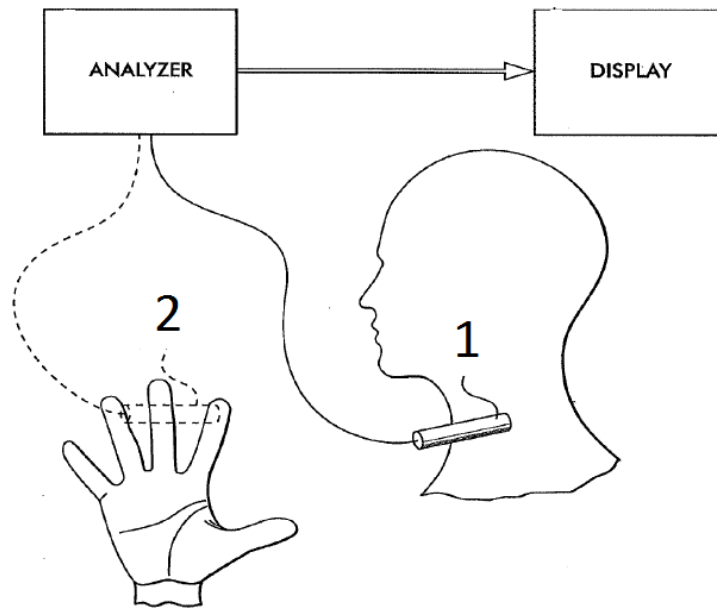
Figure 22. Measurements of blood pulse pressure using pressure sensor on the neck together with other pressure sensor's reference signal from fingers [14].

In practical part of our work it is proposed to use Electrical Bioimpedance Measurement (EBI) method to assess the blood pulse waveform. It could be an alternative method for pressure sensor measurement. This work does not include the comparable analysis of two technologies as this requires both technologies' experimental data presense. However, EBI measurements could have and advantage in such parameters as „ease of use" and "continuous measurements possibility". Nevertheless, both technologies are worth being assessed in the future and could be interchangeable or complimentary parts of developed medical device for ICP assessment.

4.3 Bioimpedance measurements theory

Electrical impedance (or simply impedance) is a measure of opposition to sinusoidal electric current. The concept of electrical impedance generalizes Ohm's law to AC circuit analysis. Unlike electrical resistance, the impedance of an electric circuit can be a complex number: $Z = V/I$, where $Z = R + jX$, and R is a real part and X is an imaginary part. Methods of measurement of electrical impedance of biological objects are in general the same, which are used in technical measurement of the electrical impedance Z.

In general, excitation signal is applied to the object and the response to this signal is measured [16]. The most common case is that excitation current is applied and voltage response is measured as on Figure 23.
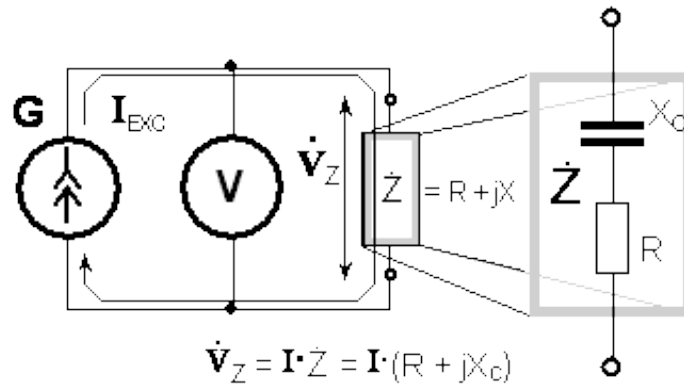

$$\dot{V}_Z = I \cdot \dot{Z} = I \cdot (R + jX_c)$$

Figure 23. Bioimpedance measurement [16].

Classically, in medicine, bioimpedance measurements are used thoracic area electrodes as it is shown on Figure 24 [15]. The measurement current is passed through the thorax in a direction parallel to spine between outer (upper) neck electrodes and high abdomen lower electrodes. The EBI measurement current produces a high-frequency voltage across the impedance of the thorax, directly proportional to impedance *Z*. This induced high-frequency voltage is sensed by two other pairs of electrodes placed inside the current path.
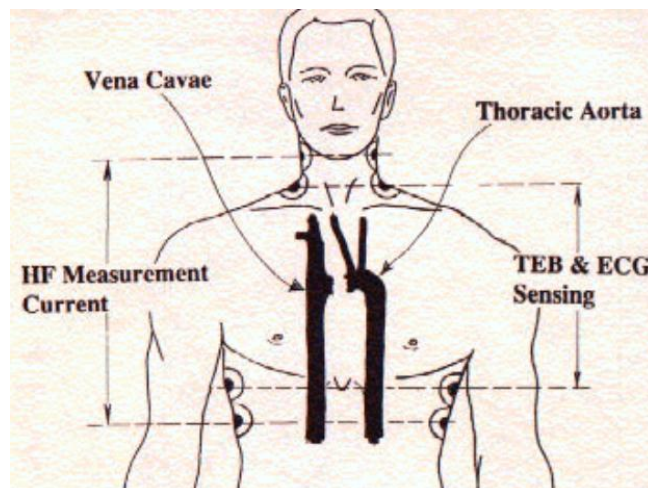

Figure 24. Location of 8 electrodes during Thoracic Electrical Bio (TEB) impedance measurements [15].

Figure 25 shows how the normal measured blood impulse looks like. Upper ECG signal is synchronized with EBI signal shown in the middle. The lower depiction is derivation from EBI signal, which is commonly used for blood pulse features analysis. It reflects such characteristics as Pre-Ejection Period (PEP) known as isovolumic contraction and Ventricular Ejection Time (VET), period that starts by opening of aortic valve and ends by its closure (S2-time). The period between systolic maximum $(dZ/dt)_{max}$ and aortic valve closure shows strong correlation with intracranial pressure regarding to Swoboda et al [14]. This means, that determining the decrease or increase of this period, we can determine the decrease or increase of ICP.
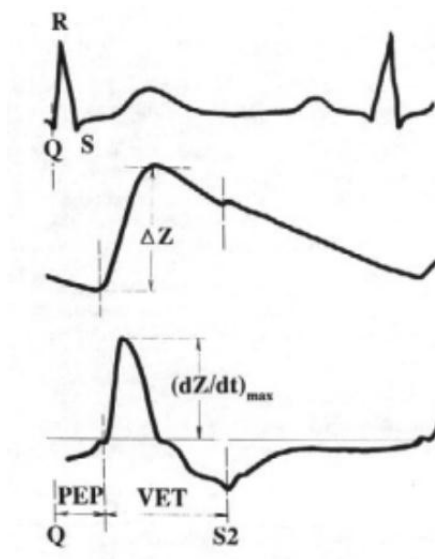

Figure 25. Timing relationship between ECG (up), ΔZ and dZ/dt signals (below) [15].

4.4 Experiments

Experiments consisted from repeated measurements of bioimpedance attaching electrodes on individual's neck. The goal of repeated measurements was:

1) Compare electrodes placement configurations;
2) Compare measurements at different frequencies;
3) Find the most steady configuration for measurements.

Configurations at different frequencies were compared by:

1) Impedance values range;
2) Ratio of blood pulse impedance to base impedance;
3) Stability of signal in repeated measurements.

4.4.1 Used tools

The measurements were done by HF2IS impedance spectroscope of Zurich Instruments with HF2TA trans-impedance amplifier [19]. These devices allow to measure the impedance of the object in the frequency range up to 50MHz using both two-electrode and four-electrode configurations.

In the experiments were used 3M Ag/AgCl foam type electrodes (Figure 26). They are commonly used in medicine for ECG measurements. These electrodes contain a layer of electrolyte fluid and a thin-film permeable membrane which is in contact with the skin. When attached to surface membrane with micro pores passes electrolyte, moisturizing the skin.

Figure 26. 3M electrodes in configuration A (horizontal 2 electrode).

4.4.2 Experimental data

Participants

Three individuals were participated in this study:

    Individual 1: Male, 28 years, 87 kg, 191 cm, BMI (Body mass index): 23,8 kg/m^2;

    Individual 2: Female 28 years, 62 kg, 175 cm, BMI: 20,2 kg/m^2;

    Individual 3: Male 29 years, 80 kg, 182 cm, BMI: 24,2 kg/m^2.

Methods

Measurements were done in configurations of 2 and 4 electrodes connections using HF2IS spectroscope and HF2TA amplifier (Figure 27).
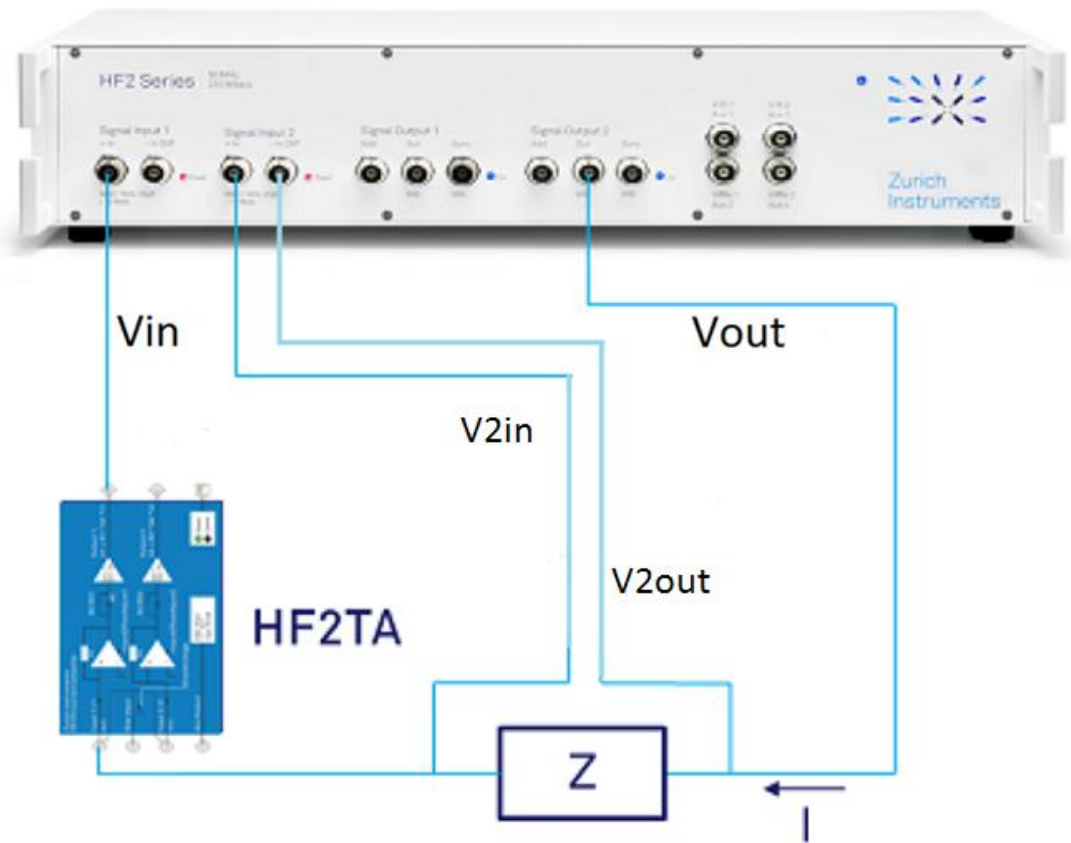

Figure 27. Impedance measurements with HF2IS spectroscope and HF2TA amplifier. Z – the object of measurement.

The impedance Z is calculated according to next equation:

$$Z = R_{\text{HF2TA}} * G * V_{2\text{in}}/V_{\text{in}} ,\qquad\qquad(2)$$

where G – total gain of current amplifier HF2TA.

Electrode placement configurations

6 different electrode placement configurations were used in experiments (Figure 28). Configurations from A to D were tested at 5 frequencies from 50 to 200 kHz.

The range of frequency was determined according to ratio of blood pulse impedance to base impedance. Configurations E and F showed significant superiority in signal quality to other configurations (discussed more in according sections below) and that became the reason for increasing measurement range for these frequencies. Instead of range 50kHz-200kHz, these configurations were measured at 8 different frequencies in range 25kHz-2MHz.

At frequencies below and above particular ranges the feasibility of blood pulse distinction from signal was not successful.

Each individual was measured at least 3 times in different days at each configuration and frequency. To summarize, more than 200 signals for configurations from A to D and more than 140 signals for E and F configurations were recorded in 12 measurement sessions.
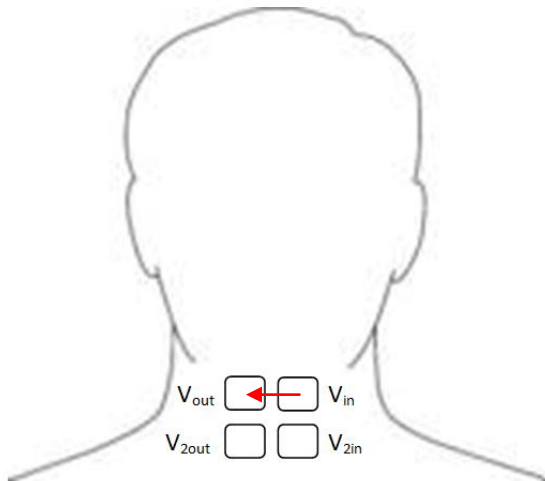
Figure 28. Electrode placement configurations. Excitation vector is marked with red arrow.
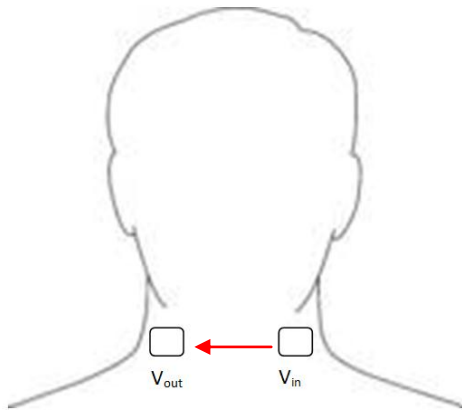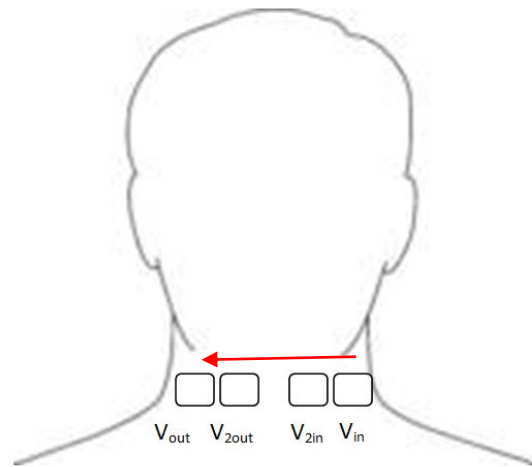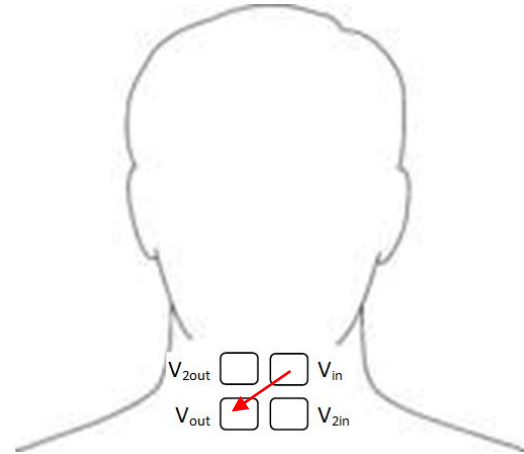

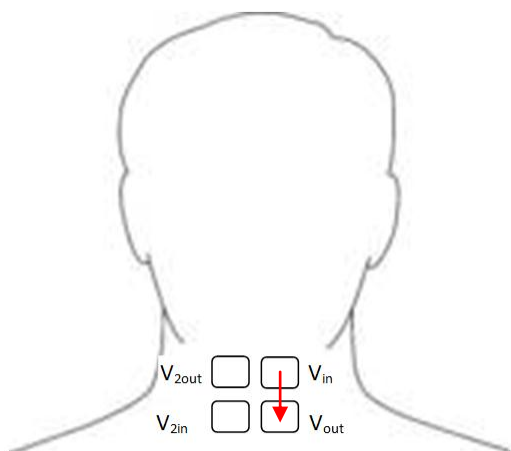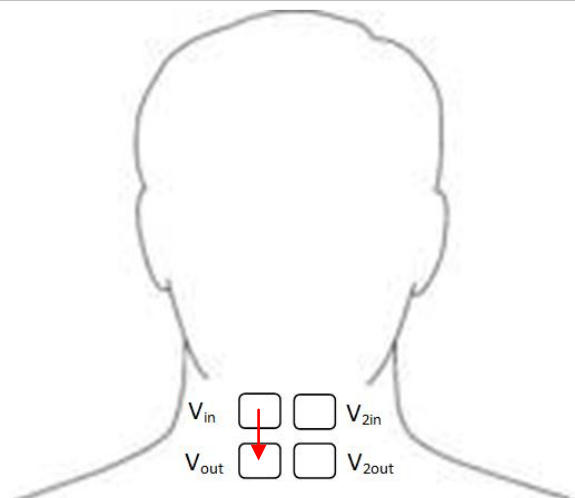|	
A. Horizontal 2	B. Horizontal 4
C. 2 Rows Up	D. 2 Rows Cross
E. 2 Rows Left Side	F. 2 Rows Right Side

4.4.3 Results

Bioimpedance and ECG correlation

To analyze bioimpedance and ECG relation short 3V 3mA DC signal was conducted through electrodes between left hand and head (Figure 28). This signal appeared as narrow peak on both, ECG and bioimpedance scales. On ECG scale it appeared right after QRS complex or the contraction of heart ventricles and on the bioimpedance scale it appeared on top of main peak ΔZ that is the pumped blood impulse.   That corresponds to synchronized ECG and bioimpedance signals on Figure 25.

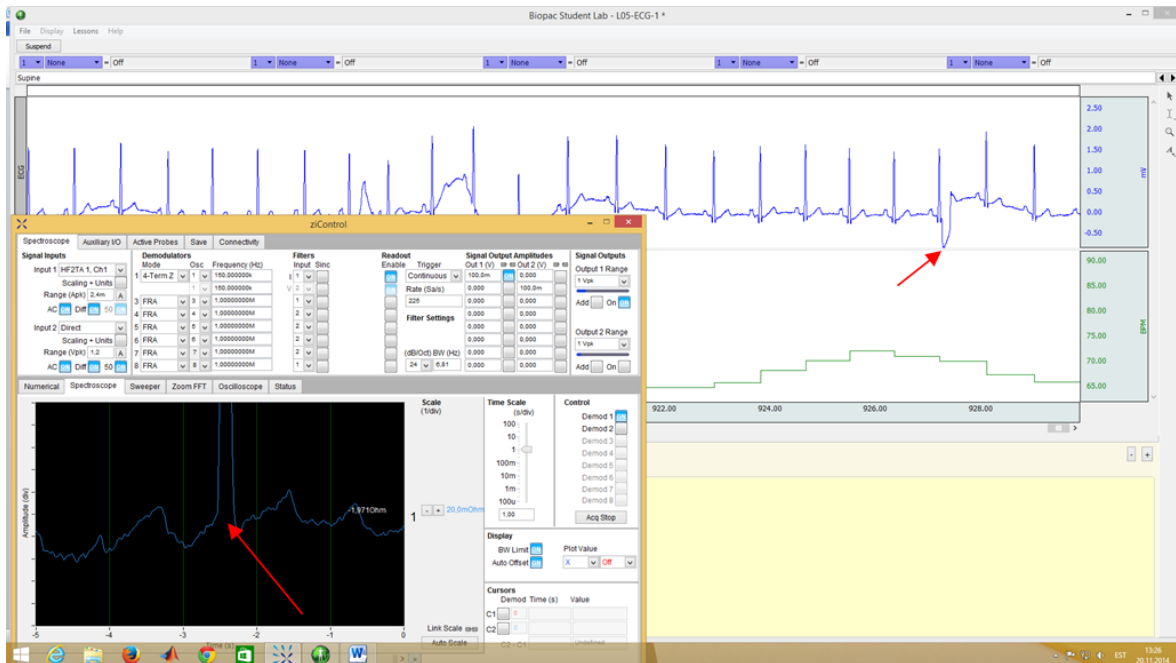*Figure 29. Impedance signal (below) and EKG signal (up) correlation. Artifact is marked with red arrow. 150 kHz signal, configuration E was used.*

Configurations A, B, C, D

Configurations A, B, C and D had significantly higher impedance value than configurations E and F (see Table 4). Difference of impedance values between 2 electrode measurements (configuration A) and 4 electrode measurements was also considerable.

Table 3.

Impedance change at different configurations

Configuration (frequency range)	Impedance range (Ohms)	Impedance range at frequency 150 kHz (Ohms)
A (50kHz-20kHz)	207 - 312.8	223-267
B (50kHz-20kHz)	13.3	15-39.7
C (50kHz-20kHz)	15.9 – 27.4	17.1-24.5
D (50kHz-20kHz)	14.8 – 24.7	16.3-21.1
E (25 kHz–300 kHz)	1.2 – 5.1	1.8-4.9
F (25 kHz–300 kHz)	1.27 - 5.2	1.4-4.7

Frequency of 200 kHz was chosen as the highest for configurations A, B, C and D. Typically signal at this frequency is influenced by respiration. In addition, some higher frequency noise (5 to 10 Hz) is seen at baseline (Figures 29, 30).
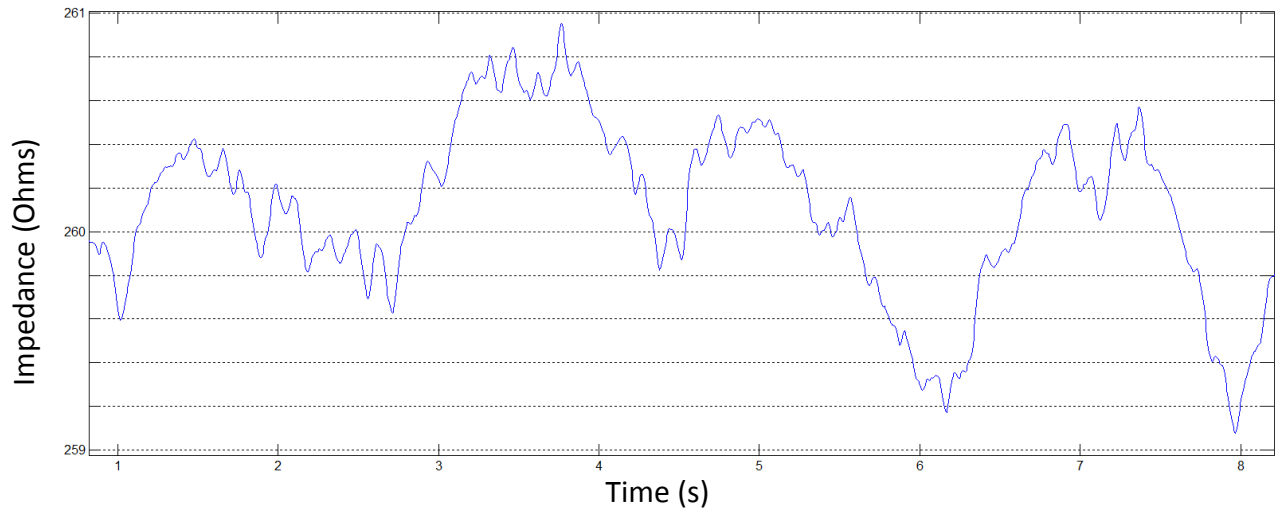
Figure 30. Typical 200 kHz signal in configuration A.
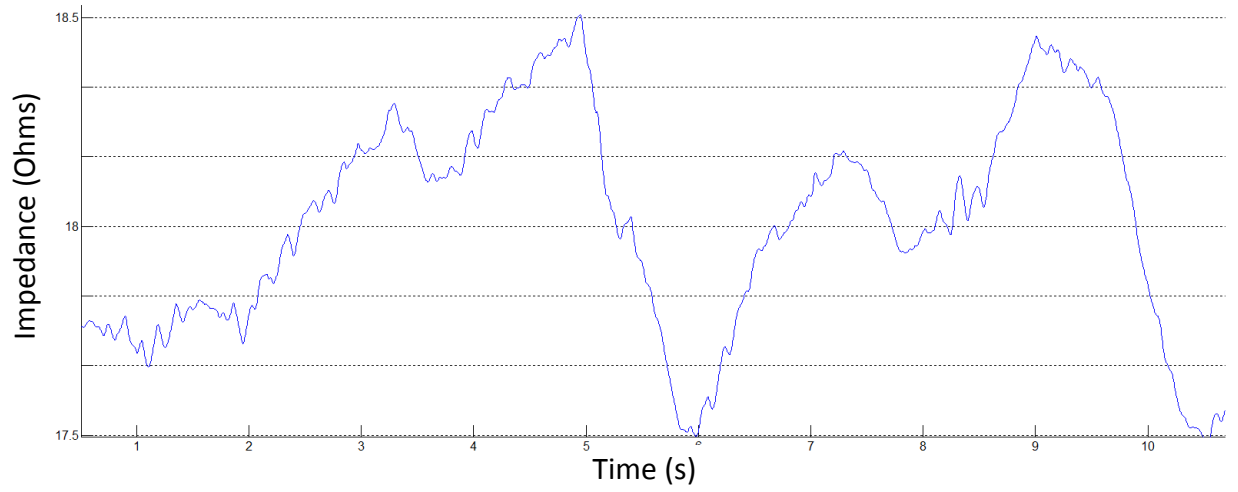
Figure 31. Typical 200 kHz signal in configuration D.

On frequencies from 50 to 150 kHz blood pulse wave shape was discernable (Figure 31).
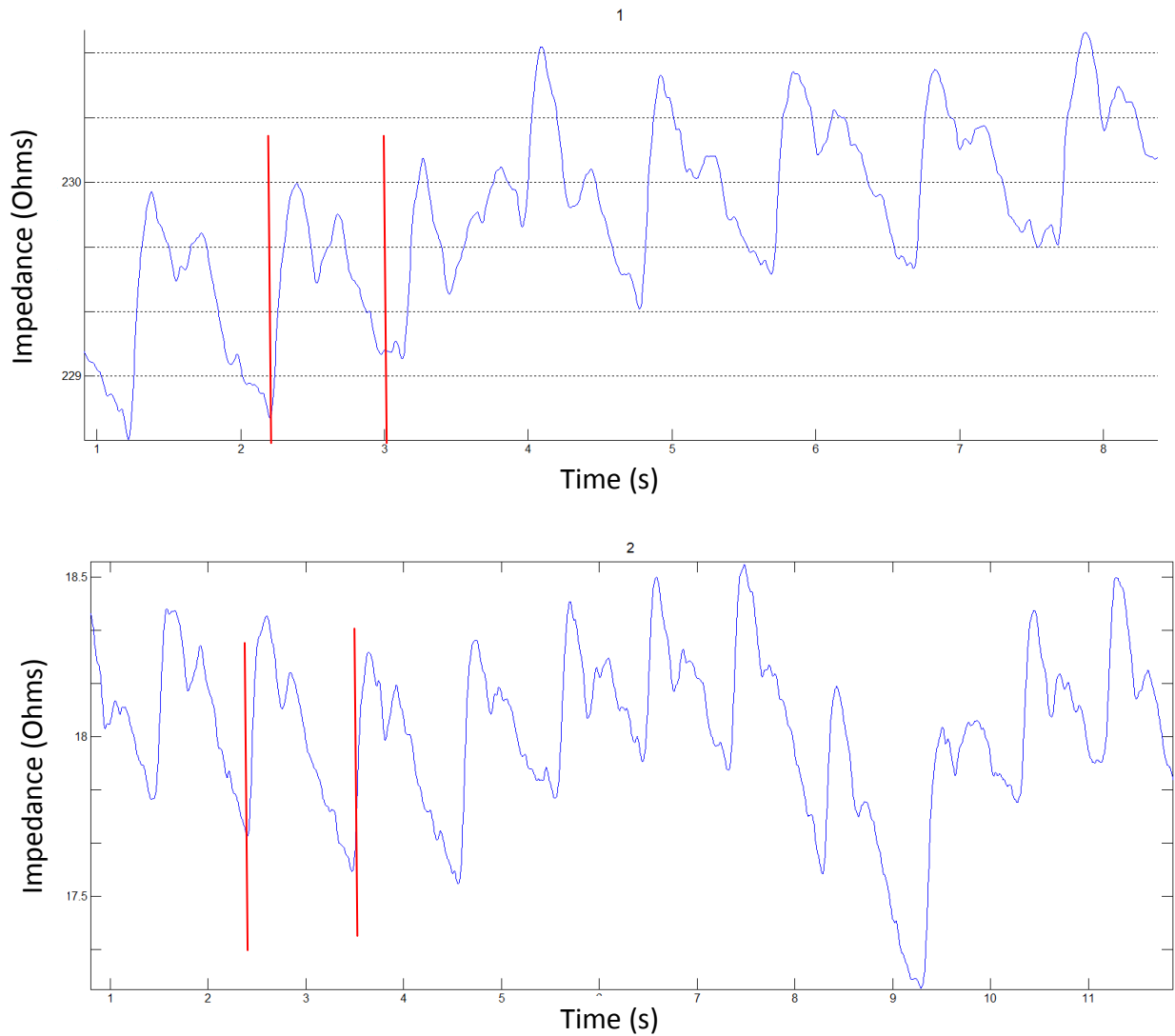
Figure 32. Impedance signals at frequency 150 kHz.1 – configuration A, 2 – configuration

B. Red brackets show blood pulse wave.

It was not possible in these trials to get clear blood pulse wave signal on configurations C and D, however both were positive to distinguish respiratory period (Figure 32).

Figure33. Impedance signals at frequency 150 kHz. 3 – configuration C, 4 – configuration D. Red brackets show respiratory period.

Configurations E & F

Configurations E and F showed better quality signal, than configurations from A to D. The superiority of signal was in:
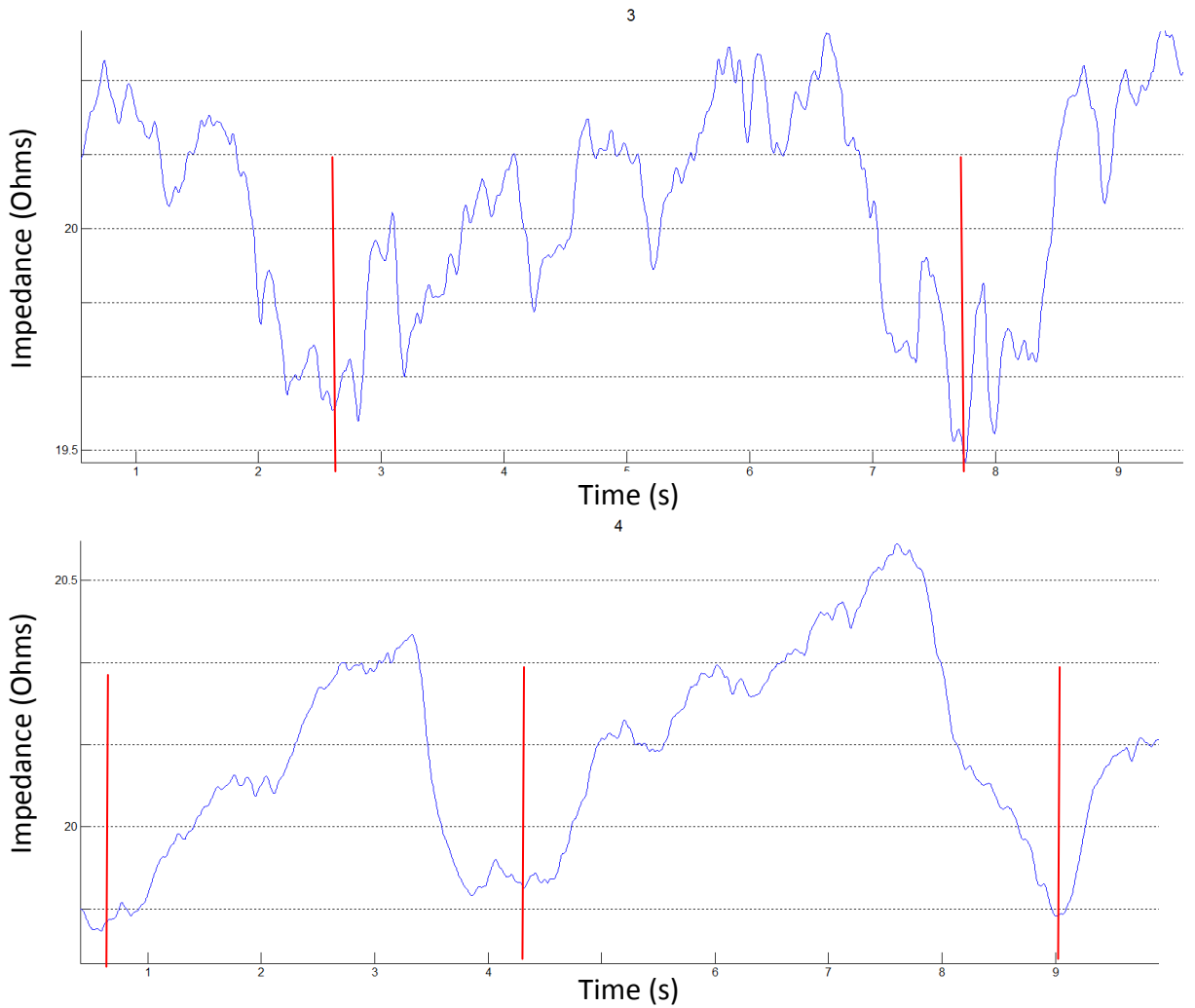
1) Blood pulse wave distinction ratio (Table 5)

2) Base impedance (also can be seen from Table 5)

3) Stability of signal at different frequencies. That became the reason to increase measurement frequency range from 50-200 kHz to 25 kHz-2 MHz.

Figure 33 shows impedance signal at frequency 2MHz. Sometimes it is possible to distinct blood pulse wave signal at this frequency, but mainly signal is disturbed by higher frequency waves (~5Hz).
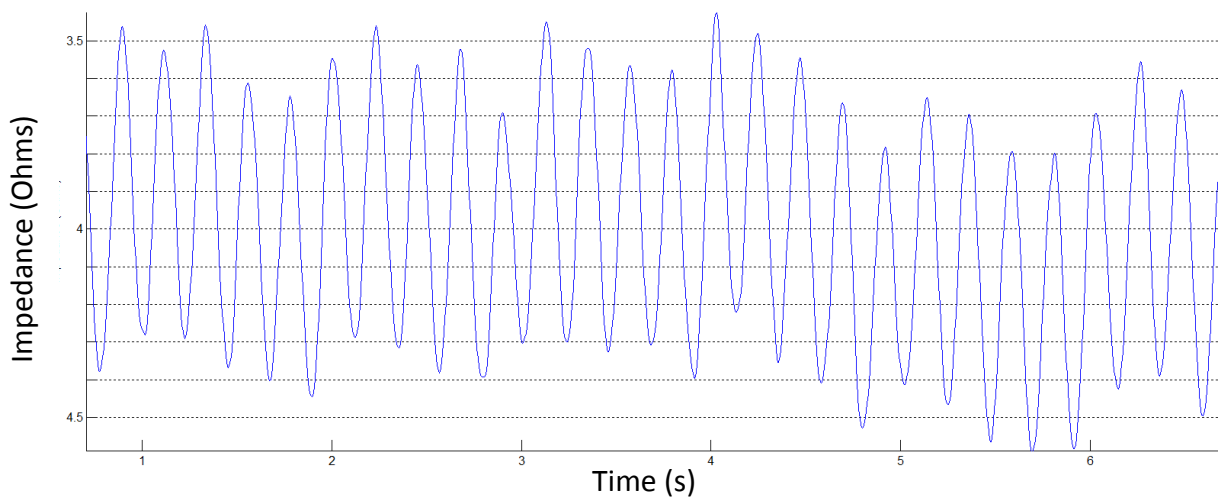
Figure 34. Typical 2MHz signal at configurations E and F. Blood pulse wave not possible to distinct

Table 4.
Basic impedance and blood pulse wave impedance ratio at f 150 kHz

Configuration	Average impedance (Ohms)	Average blood pulse wave value (Ohms)	Ratio (%)
A	247.6	0.5	0.2
B	17.1	0.02	0.1
C	19.2	0.15	0.8
D	18.6	0.1	0.5
E	2.8	0.04	1.4
F	2.8	0.04	1.4
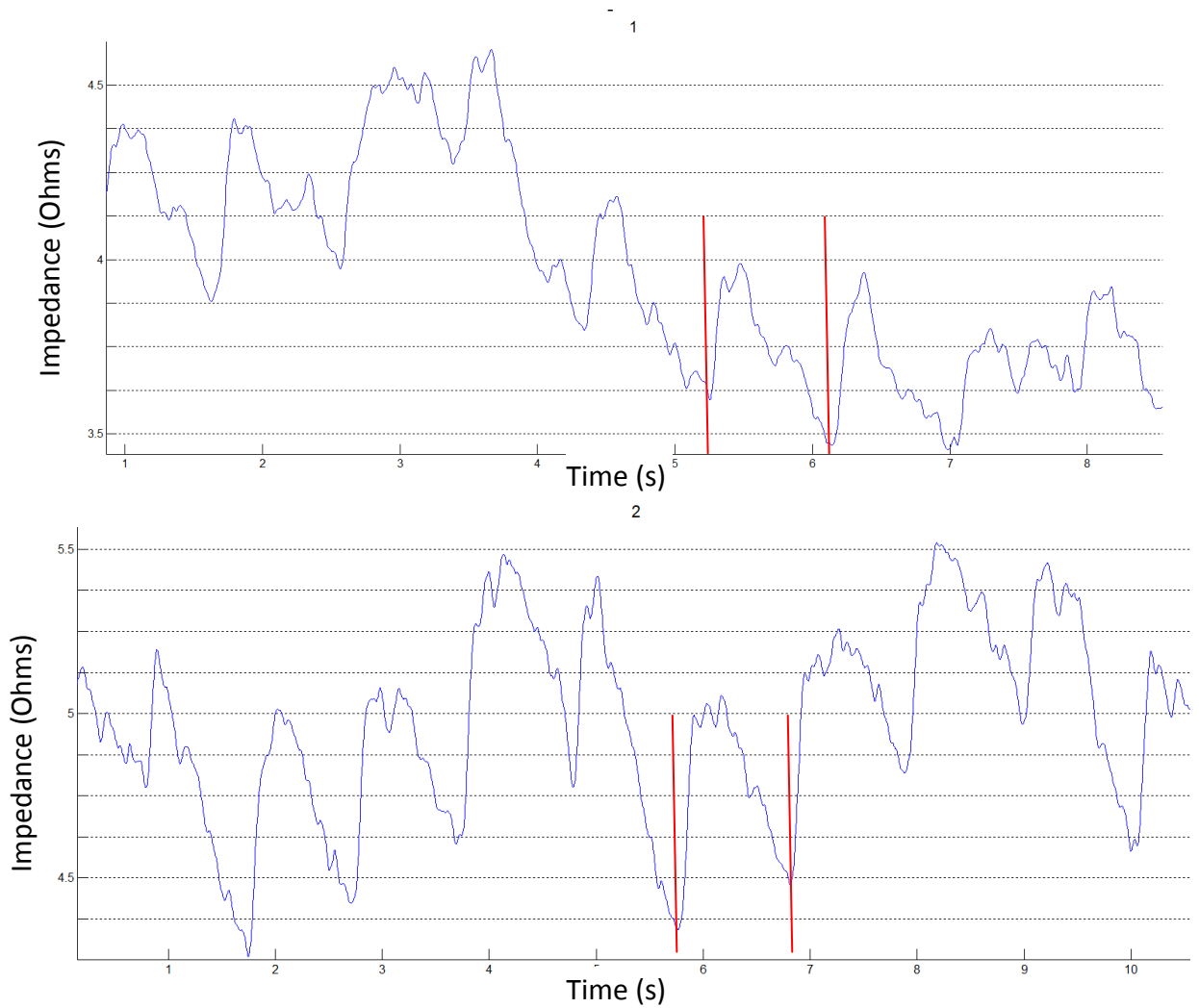
Figure 35. Signals at frequency 150 kHz.1 – configuration E, 2 – configuration F. Red brackets show blood pulse wave.

Blood Pulse Wave value

The average impedance value of blood pulse wave was 0.14 Ohms in range between 0.02 Ohms and 0.5 Ohms and it signified in 0,74% of average base impedance (Table 5).

Measurements between individuals

No significant impedance value difference between 3 individuals was found (Table 6). However, skin preparation conditions influenced impedance values significantly. Same individual impedance could change dramatically because of unprepared contact place on skin or electrodes quality. These problems are described in more details in Discussion section.

Table 5.

Impedance values between individuals at frequency 150 kHz.

Configuration	Individual 1 Impedance average (Ohms)	Individual 2 Impedance average (Ohms)	Individual 3 Impedance average (Ohms)
A	267	245.2	250.0
B	16.7	18.9	16.7
C	18.9	20.1	20.2
D	20.1	18.4	18.4
E	4.9	3.1	2.6
F	4.7	2.9	2.8

4.4.4 Discussion

During these experiments it was found that following specific rules, described below, there is a positive probability to obtain a blood pulse wave signal at configurations A, B, E and F. These rules are:

1) Electrodes V_{in} and V_{out} should be attached to palpable place on neck

2) Electrode – skin contact place should be prepared

These two circumstances appeared to be crucial for obtaining a blood pulse wave in bioimpedance measurements from neck.

Electrodes have to be attached on palpable place on the neck. The distinction of blood wave shape is better in this case (Figure 35). In case of improper placement of electrodes, for example too far from palpable places, it becomes difficult to distinguish the shape of blood wave from other potentials like muscles movement or respiration (Figure 36).
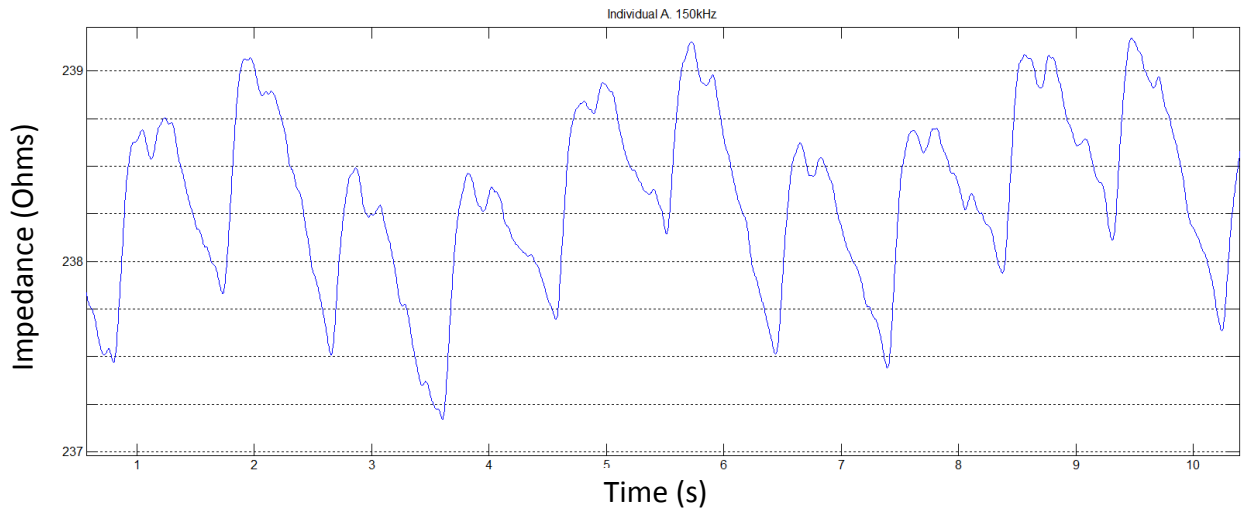
Figure 36. 2 electrodes measurement (configuration A). Electrodes are fitted properly on palpable areas on the neck. Heart wave shape is positively distinctive.
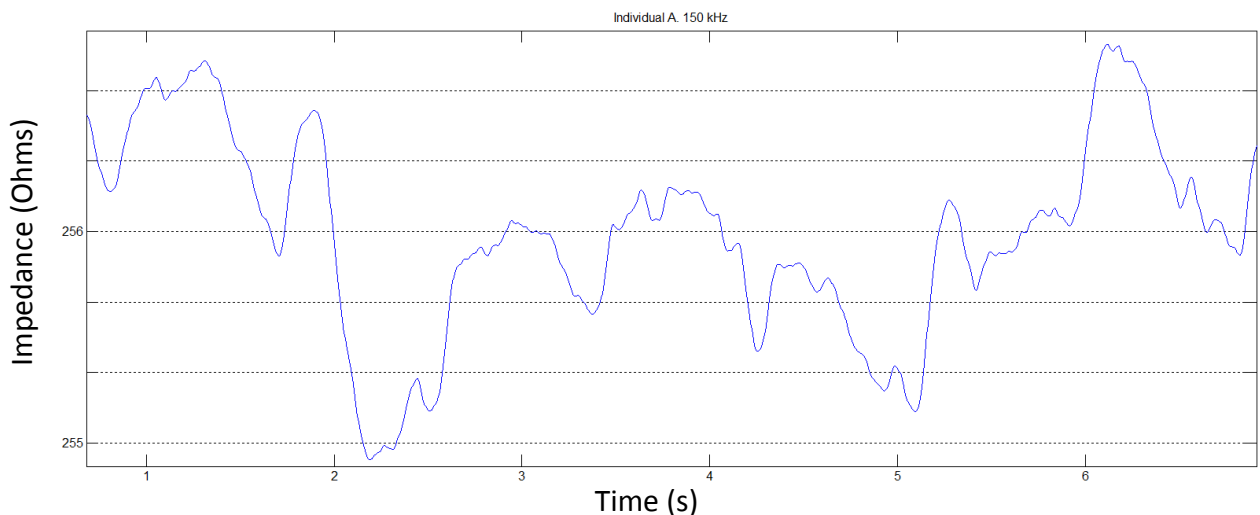
Figure 37. 2 electrodes measurement (configuration A). Electrodes are placed too far from palpable areas on the neck. Heart wave shape is hardly distinctive.

Contact between electrodes and skin. Although, there were no significant difference between individuals' impedance data (Table 7), electrodes – skin contact can play significant role on measurements. For example, depending on next factors, impedance can dramatically change in different measurements.

1) skin preparation (removal of hairs, fat, dirt etc)
2) electrodes' contact area freshness (when were unpacked, storage conditions)

In next Table a comparison is done to show how considerably the impedance value changes if skin preparation is not appropriate. In first column there are shown measurements of individual 3 having 1 day's stubble   on his neck. In second column

there are shown measurements of the same individual after shaving. A regular razor blade was used for shaving. The cleaning with disinfectant of particular skin area was applied after the shaving.

Table 6.

Influence of skin preparation on impedance value. Individual 3, electrodes configuration E

Frequency	Impedance of unshaved (unprepared) skin (Ohms)	Impedance of shaved (prepared) skin (Ohms)	Difference (%)
25 kHz	30.5	4.4	693.2
75 kHz	29.2	4.7	621.3
150 kHz	32	4.9	653.1
300 kHz	50.8	5.1	996.1
500 kHz	67.1	5.14	1305.4
1000 kHz	88	4.8	1833.3
1500 kHz	109	4.06	2684.7
2000 kHz	122	4.9	2489.8

CONCLUSION

In the theoretical part of this work the human brain structure and main functions were described. An overview of traumas and pathologies related to increased intracranial pressure (ICP) was given. Additionally, existing methods of invasive and noninvasive ICP measurements were briefly discussed.

In the practical part of this work the relationship between ICP and EBI measurement of blood pulse wave was discussed. A similar project with using a pressure sensor for ICP assessment was described. The theoretical possibility of using EBI measurements for ICP assessment was explained.

An experiment with EBI measurements of the blood pulse waveform was conducted. Three individuals were tested at different frequencies using various electrode placement configurations. The measurement results are compared at different configurations and frequencies. Configurations E and F (see Figure 28) at a frequency range between 25 kHz and 2 MHz were considered the best configurations for obtaining of blood pulse wave. No significant impedance value change between individuals was noticed.

The purpose of the experiment was to ascertain whether it is possible to distinguish the blood pulse wave from carotid arteries using bioimpedance measurements in repeated evaluations. Not only was the possibility of distinguishing a blood pulse waveform was confirmed, but also some considerable findings were discovered. These are the importance of skin preparation and the freshness of the electrodes' contact area.

A noninvasive ICP measurement tool is in high demand today. In this field the first steps are being made for new technology development. Similar technology using a pressure sensor instead of EBI is already patented and was described briefly in this work. EBI measurements could have an advantage in such parameters as "ease of use" and "the possibility of continuous measurements". Nevertheless, both technologies are worth being assessed in the future and could be interchangeable or complimentary parts of a developed medical device for ICP assessment. These next steps could be considered useful for this technology's development:

- Confirmation of a relationship between ICP and blood pulse waveform in carotid arteries in large studies involving patients with increased ICP;
- Investigation of the reflection part in blood pulse waveform in carotid arteries using EBI measurement.

References

[1] Gerard J. Tortora, Mark T. Nielsen. "Principles of Human Anatomy ". 12th edition. R. R. Donneley, 2010, 1056 pages.

[2] J-M. Le Minor, H. Sick. "Bourgery. Atlas of Human Anatomy and Surgery ". Vol. 1. Original Edition. Taschen, 2008, 722 pages.

[3] D. Shier. "Hole's Human Anatomy and Physiology". 12th edition. McGraw-Hill, 2010, 978 pages.

[4] "Brain and Nervous System". Available at: http://www.webmd.com/brain. [WWW], (20.10.2014).

[5] London M. "Influence of arterial pulse and reflected waves on blood pressure and cardiac function". Am Heart J, 1999 Sep, 138(3 Pt 2):220-4.

[6] R. Rubin, D. S. Strayer. "Rubin's pathology". 6th edition. Lippincott Williams & Wilkins, 2012, 1466 pages.

[7] E. Goljan. "Rapid Review Pathology". 4th edition. Saunders, 2013, 784 pages.

[8] Donnan et al. "Stroke". Lancet, May 2008, 371 (9624): 1612–23.

[9] W. Dorland, "Dorland's Illustrated Medical Dictionary". 32nd edition. Saunders, 2011, 2176 pages.

[10] H. Royden Jones Jr. Jr. et al. "Netter's Neurology". 2nd edition. Saunders, 2011, 768 pages.

[11] P. H. Raboel et al. "Intracranial Pressure Monitoring: Invasive versus Non-Invasive Methods - A Review". Critical Care Research and Practice. Volume 2012, Article ID 950393, 14 pages

[12] "Oral & maxillo-facial surgery". Available at:
http://oralmaxillo-facialsurgery.blogspot.com/2010/05/middle-ear-tympanic-membrane.html. [WWW], (20.10.2014).

[13] "Optic Nerve". Available at: http://www.webmd.com/eye-health/optic-nerve. [WWW], (20.10.2014).

[14] M. Swoboda et al. "Non-invasive intracranial pressure sensor". Patent Application Publication, US, 2913/0289422.

[15] W.G.Kubicek. "On the sourse of peak first time derivative (dz/dt) during impedance cardiography". Annals of Biomedical Engineering. Vol.17. 1989, pp.459-462.

[16] Methods and means for measurement of electrical bioimpedance. Available at: http://www.elin.ttu.ee/mesel/Study/Subjects/9010_TFI/Contents/BImeasur/Index.htm. [WWW], (20.10.2014).

 [17] Niccomo datasheet, Medis GmbH. Available at: http://www.medis-de.com. [WWW], (20.10.2014).

 [18] Marmarou et al. "A nonlinear analysis of the cerebrospinal fluid system intracranial pressure dynamics". J Neurosurg, 1978, 48:332-344,.

[19] Zurich Instruments. "HF2 User Manual". 2014. Available at: http://www.zhinst.com/manuals/hf2. [WWW], (20.10.2014).

[20] "Orsan. Executive Summary", 2013. Available at: http://www.orsan-medical.com. [WWW], (20.10.2014).

Appendix 1
Major parts of the brain [3].

Part	Characteristics	Functions
Cerebrum	Largest part of the brain; two hemispheres connected by the corpus callosum	Controls higher brain functions, including interpreting sensory impulses, initiating muscular movement, storing memory impulses, initiating muscular movements, storing memory, reasoning, and determining intelligence
Basal nuclei (ganglia)	Masses of gray matter deep within the cerebral hemispheres	Relay stations for motor impulses originating in the cerebral cortex and passing into the brainstem and spinal cord
Diencephalon	Includes masses of gray matter (thalamus and hypothalamus)	The thalamus is a relay station for sensory impulses ascending from other parts of the nervous system to the cerebral cortex; the hypothalamus helps maintain homeostasis by regulating visceral activities and by linking the nervous and endocrine systems

Appendix 1 continues

Brainstem		Connects the cerebrum to spinal cord	
	Midbrain	Contains masses of gray matter and bundles of nerve fibers that join the spinal cord to higher regions of the brain	Contains reflex centers that move the eyes and head, and maintains posture
	Pons	A bulge on the underside of the brainstem that contains masses of gray matter and nerve fibers	Relays nerve impulses to and from the medulla oblongata and cerebrum; helps regulate rate and depth of breathing
	Medulla oblongata	An enlarged continuation of the spinal cord that extends from the foramen magnum to the pons and contains masses of gray matter and nerve fibers	Conducts ascending and descending impulses between the brain and spinal cord; contains cardiac, vasomotor and respiratory control centers and various nonvital reflex control centers
Cerebellum		A large mass of tissue located below the cerebrum and posterior to the brainstem; includes two lateral hemispheres connected by the vermis	Communicates with other parts of the CNS by nerve tracts; integrates sensory information concerning the position of body parts; and coordinates muscle activities and maintain posture